HHS Public Access

Author manuscript

Org Biomol Chem. Author manuscript; available in PMC 2017 July 07.

Published in final edited form as:

Org Biomol Chem. 2016 July 07; 14(25): 5894–5913. doi:10.1039/c6ob00878j.

Total Synthesis, Biosynthesis and Biological Profiles of Clavine Alkaloids

Stephanie R. McCabe[a] and **Peter Wipf**[a]

[a]Department of Chemistry, University of Pittsburgh, Pittsburgh, PA, 15260, U.S.A

Abstract

This review highlights noteworthy synthetic and biological aspects of the clavine subfamily of ergot alkaloids. Recent biosynthetic insights have laid the groundwork for a better understanding of the diverse biological pathways leading to these indole derivatives. Ergot alkaloids were among the first fungal-derived natural products identified, inspiring pharmaceutical applications in CNS disorders, migraine, infective diseases, and cancer. Pergolide, for example, is a semi-synthetic clavine alkaloid that has been used to treat Parkinson's disease. Synthetic activities have been particularly valuable to facilitate access to rare members of the Clavine family and empower medicinal chemistry research. Improved molecular target identification tools and a better understanding of signaling pathways can now be deployed to further extend the biological and medical utility of Clavine alkaloids.

Graphical Abstract

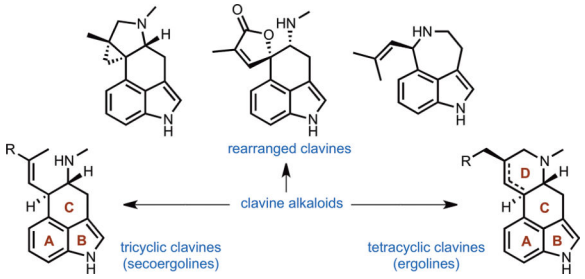

1. Introduction

The clavine alkaloids are a subclass of the ergot family of indole-containing alkaloids produced by several members of the *Clavicipitaceae* and *Trichocomaceae* families of filamentous fungi. Historically, ergot alkaloids have had a long-lasting and significant impact on both human health and agriculture. They were first documented as notorious poisons, stemming from the Middle Ages in central Europe where consumption of ergot alkaloid contaminated cereal grains led to epidemics of ergotism or St Anthony's fire resulting in tens of thousands of fatalities.[1] Two forms of ergotism are recognized clinically: convulsive ergotism is characterized by hallucinations, convulsions and fever, whereas gangrenous ergotism is characterized by gangrene of the feet, legs, hands and arms.[2] Ergotism in humans is now rare due to strict guidelines governing the acceptable concentration of ergot alkaloids in grain. However, ergotism can still cause serious epidemics in livestock.[3,4] The presence of ergot in commercial cereal crops continues to

represent a significant problem that can result in huge economic loss when contaminated harvests are downgraded or discarded. Susceptible host plants include cultivated cereals like rye, wheat, triticale, barley and oats as well as several species of wild grasses.[4] Infection of the host plant is characterized by the replacement of healthy seeds or kernels with dark coloured sclerotia, which contain a variety of ergot alkaloids. The sclerotia are the resting state of the fungus allowing it to survive harsh conditions over winter. In spring, moisture stimulates germination of the sclerotia into stromata, which undergo meiosis and produce fruiting bodies called perithecia. The perithecia release ascospores that are disseminated to host plants by wind currents where they invade the plant's ovaries. Conidia are formed and exuded as honeydew that attracts insects, thereby facilitating transmission to other plants. The fungus then matures into sclerotia and the infection process is repeated.[5,6] Ergot is particularly common in temperate climates but can also occur in subtropical and arctic regions and is particularly severe in seasons when cold, wet weather optimal for sclerotia germination coincides with flowering crops.[3,4,5,7] The fungus-host relationship is typically classified as parasitic because the fungus depletes the host plant of essential nutrients and directly causes seed loss.[7] However, the plant can acquire several ecological benefits from harboring the fungus, which may in some cases compensate for the detrimental parasitic properties. These include protection from predation through the fungus' production of toxic ergot alkaloids, as well as increased drought resistance and improved growth and nutrient uptake.[8] Modern control of ergot is focused on limiting the presence of sclerotia through preventative measures such as crop rotation, field burning post harvest and the use of fungicides.[5] Contaminated crops can be saved by separating the ergot kernels from cereal grains based on density or colour prior to milling.[3]

2. Biosynthesis & Classification

2.1 Biosynthesis

Significant progress has been made in the identification and characterization of genes responsible for the biosynthesis of clavine alkaloids. Initial advances were largely achieved through isotope labeling experiments and gene disruption studies followed by gene product expression and characterization.[8] More recently, the identification of ergot alkaloid synthesis (*eas*) gene clusters has enabled heterologous expression of entire biosynthetic pathways in a suitable host strain, greatly facilitating the elucidation of mid to late pathway genes.[9,10,11] The tendency of pathway genes to cluster in close proximity on the genome is characteristic of secondary metabolite pathways in filamentous fungi. Clustering is believed to confer a selective advantage, possibly through improved gene regulation or as a mechanism to facilitate horizontal gene transfer.[9,12] The first five genes in the biosynthetic pathway are responsible for the formation of the tricyclic core. These genes are common to all ergot alkaloids and their functions have been assigned to reaction steps from L-tryptophan to chanoclavine-I aldehyde (**10**). The first step in the pathway is an electrophilic aromatic substitution of dimethylallyl pyrophosphate (DMAPP) at the C(4) position of L-tryptophan (**3**) to produce 4-dimethylallyltryptophan (4-DMAT) (**4**) (Figure 1). *N*-methylation of the amino group is catalysed by an *easF* derived *N*-methyltransferase in the presence of an *S*-adenosyl methionine (SAM) cofactor to deliver *N*-methyldimethylallyltryptophan (*N*-Me-DMAT) (**5**) which can be converted into chanoclavine-I (**9**) through a series of oxidation,

decarboxylation and cyclisation reactions. While the precise enzymatic mechanism of these transformations is unknown, *easC* and *easE* have been identified as the genes responsible for this sequence as deletion mutations of *easC* and *easE* accumulate *N*-Me-DMAT.[13,14] Oxidation of chanoclavine-I generates chanoclavine-I aldehyde (**10**) the last common biosynthetic precursor of all ergot alkaloids. While the first five steps are conserved in most species of fungi, additional structural diversity can be generated via short diverted 'shunt' pathways. Clavicipitic acid (**1**) is proposed to arise from 4-DMAT through benzylic oxidation and aminocyclisation.[15] Subsequent decarboxylation yields aurantioclavine (**2**).[16] While the precise mechanism for the formation of rugulovasines A (**11a**) and B (**11b**) is unknown, they were isolated along with chanoclavine-I (**9**) and could conceivably originate from an oxidative cyclisation of chanoclavine-I.[17]

From chanoclavine-I aldehyde (**10**) on, the biosynthetic pathway diverges and late pathway enzymes responsible for functionalizing the ergoline core catalyse a series of lineage specific steps to produce a diverse profile of clavine alkaloids. Clavine producers typically generate multiple alkaloid products rather than a single pathway end product. This is due in part to variable late stage derivatization patterns in different species of fungi as well as the accumulation of intermediates and alternate products along the pathway in concentrations that can be comparable to the pathway end products.[10,18,19] Recent studies by O'Connor and Panaccione suggest that the branch point in clavine alkaloid biosynthesis is controlled by different isoforms of the enzyme encoded by *easA*.[20,21] In *Clavicipitaceae* fungi, *easA* encodes an isomerase that converts chanoclavine-I aldehyde (**10**) into agroclavine (**16**) by E/Z isomerization to form enal **14**, followed by spontaneous cyclisation and *easG* mediated reduction (Figure 2). Agroclavine (**16**) can then go on to form a series of related clavine alkaloids characterized by the presence of a double bond in the D-ring and ultimately form lysergic acid (**18**). Alternatively, in *Trichomaceae* fungi, *easA* is proposed to encode a reductase and catalyse the conjugate reduction to form aldehyde **19**, which can then spontaneously cyclize to form iminium ion **20**. This iminium ion can either be reduced to yield festuclavine (**21**) or tautomerize to the corresponding enamine **25**. The diverted clavine alkaloid cycloclavine (**26**) is formed when enamine **25** undergoes an oxidative cyclopropanation catalysed by an *easH*-derived dioxygenase followed by reduction of the resulting iminium ion. This pathway is supported by the coisolation of cycloclavine (**26**) and festuclavine (**21**), indicating that the gene cluster produces a mixture of these two compounds in the native host.[11] Festuclavine (**21**) can be converted into fumigaclavine A (**23**), B (**22**), and C (**24**), the pathway end products, through a series of oxidation, acetylation and prenylation reactions.

2.2 Classification

Clavine alkaloids can be broadly grouped into tetracyclic, tricyclic or rearranged subclasses according to their structures and biosynthetic origins (Figure 3). Tetracyclic clavine alkaloids are the most numerous and possess a characteristic ergoline core. These alkaloids are typically late-stage intermediates or end products of the biosynthetic pathway. They differ in the presence or absence of a double bond in the D-ring and in the oxidation state of the C(8) substituent, which is typically at the alcohol or alkane oxidation level. Tricyclic clavine alkaloids lack a cyclized D-ring and are mostly intermediates in the biosynthesis of

more complex tetracyclic clavine alkaloids. Lastly, rearranged clavine alkaloids contain a modified ergoline scaffold with different connectivity compared to classic tricyclic and tetracyclic clavines. These alkaloids are products of diverted 'shunt' pathways apart from the primary biosynthetic pathway that leads to tetracyclic clavines.

3. Synthetic approaches to rearranged clavine alkaloids covering: 2001–2016

3.1 Aurantioclavine

Aurantioclavine (**2**) was first isolated in 1981 from the fungus *Penicillium aurantiovirens*.[22] It has become an attractive target for total synthesis campaigns due to the intriguing synthetic challenge posed by the fused azepinoindole core and its role as a biosynthetic precursor to the communesin alkaloids, which display cytotoxicity against leukemia cell lines.[23] Several groups have succeeded in preparing aurantioclavine (**2**) in racemic and enantiomerically enriched forms. Taking advantage of the innumerable methods now available for forming functionalized anilines and indoles, most modern syntheses focus on strategies to form the chiral azepine ring from one of the aforementioned pre-functionalized heterocycles. These synthetic strategies are summarized in five recent synthetic routes.

3.1.1 Enantioselective total synthesis of (−)-aurantioclavine by oxidative kinetic resolution (OKR)/ Mitsunobu ring closure—In 2008, Stoltz and coworkers accomplished the first asymmetric total synthesis of (−)-aurantioclavine (**2**).[24] Their retrosynthetic strategy relied on a late-stage Mitsunobu reaction to close the azepine ring through N(6)-C(5) bond formation from indole **27**, followed by dehydration of the tertiary alcohol to the olefin (Figure 4). The requisite 3,4-disubstituted indole precursor **27** could conceivably be obtained through a Stille cross-coupling at the C(3) position of indole **28**, followed by a hydroboration-oxidation sequence. The enantiomerically enriched amino alcohol **28** could be accessed by a strategic Pd-catalysed OKR of benzylic alcohol **29** followed by a Mitsunobu inversion. Alcohol **29** in turn could be obtained from the known aldehyde **30**. At the outset of this synthesis, the absolute configuration at the sole stereocenter at C(7) had not yet been elucidated. An X-ray analysis of an advanced synthetic intermediate *en route* to (−)-aurantioclavine subsequently assigned it as (7*R*).[25]

Following a 1,2-addition of the dianion of isobutylene oxide to aldehyde **30**, the resulting racemic alcohol **29** was subjected to Pd-catalysed OKR conditions, exploiting the use of (−)-sparteine as the chiral ligand and O_2 as the stoichiometric oxidant (Scheme 1).[26] Gratifyingly, benzylic alcohol **29** proved an excellent substrate for the OKR, delivering enantiomerically enriched alcohol **33**, derived from the more slowly reacting enantiomer, in 37% yield and 96% ee. Ketone **32**, formed by oxidation of the more rapidly reacting enantiomer, was readily recycled by $LiAlH_4$ reduction in 95% yield. Mitsunobu inversion of secondary alcohol **33** upon treatment with hydrazoic acid afforded the corresponding chiral azide, setting the requisite (*R*)-configuration at C(7). Conducting the reaction at low temperature proved to be essential in order to minimize racemisation of the configurationally labile stereogenic benzyl carbon. Hydrogenation of the azide and nosyl protection of the resulting amine afforded sulfonamide **28**. Subsequent bromination at the C(3) position of

indole **28** followed by Stille coupling with tributylvinyltin proceeded smoothly to furnish vinyl indole **34**. Next, an attempt was made to introduce the trisubstituted olefin required in the natural product, and, after screening a number of conditions, dehydration of tertiary alcohol **34** was ultimately achieved using phosphorus oxychloride in pyridine. The desired olefin **35** was obtained as the major product along with minor amounts of regioisomer **36**. With key intermediate **35** in hand, attention turned to the final challenge, closing the azepine ring. Regioselective hydroboration-oxidation of the terminal olefin furnished the protected amino alcohol **37**, which smoothly underwent annulation to azepine **38** when subjected to Mitsunobu conditions. Removal of the two sulfonamide protecting groups completed the total synthesis of (−)-aurantioclavine in 13 linear steps and <1% overall yield from **30**.

3.1.2 Total synthesis of (±)-aurantioclavine by Pictet-Spengler condensation— An elegant total synthesis of aurantioclavine (**2**) by the Ishikura group featured a striking application of the Pictet-Spengler condensation in natural product synthesis.[27] Completed in just 3 linear steps and 21% overall yield from readily accessible starting materials, it represents the shortest total synthesis to date. The authors anticipated that the natural product could be obtained from the pivotal 5-hydroxy indole derivative **39**, which should be well-suited for further deoxygenation (Figure 5). The astonishing brevity of the synthesis originates from the strategic Pictet-Spengler disconnection, which forges the azepinoindole ring in compound **39** in a single transformation from *N*-benzylserotonin (**41**) and 3-methylbutenal (**40**).

The base-promoted azepine formation was initiated by condensation of *N*-benzylserotonin **41** with aldehyde **40** to form an iminium ion intermediate **42**, which was trapped by nucleophilic attack of the pendant indole (Scheme 2). The crude product was immediately subjected to a triflation reaction, thereby forming the fully functionalized azepinoindole core **43** in 60% yield. The unusual regioselectivity observed in the Pictet-Spengler reaction can be attributed to the presence of the 5-hydroxy group, which presumably aids in directing nucleophilic attack through the C(4) position of indole rather than C(2). Following the successful installation of the azepine ring, completion of the synthesis required a selective cleavage of the triflate and benzyl protecting groups in the presence of the reductively labile isobutenylamine moiety. Exposure of compound **43** to standard catalytic hydrogenation conditions of 10% Pd/C and H_2 (1 atm) in MeOH proved too harsh and resulted in an exclusive formation of the over-reduced product **44**. Milder catalytic hydrogenation transfer conditions on **43** (10% Pd/C in the presence of HCO_2NH_4) led to aurantioclavine (**2**) in 35% yield along with benzylamine **39** and over-reduced amine **44** in 18% and 28% yield, respectively. Triflate cleavage of the partially reduced benzylamine **39** at 100 °C in the presence of formic acid, $PdCl_2(PPh_3)_2$, dppp and NEt_3 provided additional aurantioclavine (**2**), thus increasing the overall yield to 26%.

3.1.3 Enantioselective total synthesis of (−)-aurantioclavine by asymmetric alkenylation/ S_N2-type annulation— In 2010, Ellman and Brak reported a concise enantioselective synthesis of (−)-aurantioclavine that capitalized on the asymmetric addition of an organoboron reagent to a chiral imine to set the absolute configuration of the secondary amine at C(7).[28,29] They envisaged that sulfinamide **46** could be elaborated into

the natural product **2** *via* an S_N2-type annulation followed by cleavage of the sulfinyl auxiliary in the resulting azepine **45** (Figure 6). Stoltz utilized a similar S_N2 strategy for the late stage installation of the azepine ring in his earlier synthesis. The requisite cyclisation precursor **46** could be generated by a key asymmetric alkenylation reaction of *N-tert*-butanesulfinyl imine **47** that could in turn be accessed by formylation of **48**.

The execution of this strategy used a palladium-catalysed formylation of 4-bromotryptophol (**48**) under modified Beller conditions (Scheme 3). *In situ* protection of the alcohol with TMSCl was crucial for the success of this sequence and avoided the formation of an undesired lactone byproduct. The resulting aldehyde **49** was directly converted into the corresponding *N-tert*-butanesulfinyl imine **47** followed by bis-tosylation to produce indole **51**. The key diastereoselective addition of the MIDA boronate **52** to the *N-tert*-butanesulfinyl imine **51** afforded the desired addition adduct **53** in 78% yield and 97:3 *dr*. Tosylate **53** is activated toward an S_N2 cyclisation, and, upon exposure to NaH, ring closure formed azepine **54** in 85% yield. The overall synthesis was completed in 6 steps and 27% yield by sequential cleavage of the sulfinamide group with HCl in MeOH followed by Mg/MeOH mediated tosyl group removal. A second slightly modified approach used a vinyl Grignard reagent instead of a vinylborane and gave a lower *dr* of 81:19 but a slightly higher overall yield of 29% in 5 steps.

3.1.4 Enantioselective total synthesis of (−)-aurantioclavine by asymmetric allylic amination—The first catalytic asymmetric total synthesis of (−)-aurantioclavine by the Takemoto group features a late-stage formation of the indole core from a highly functionalized benzannulated azepine **55** and utilizes an asymmetric allylic amination reaction.[30] The authors anticipated that (−)-**2** could be obtained from alkene **56** *via* a cross-metathesis reaction with Grubbs' 2nd generation ruthenium catalyst to install the isobutenyl group, followed by indole closure through the N(1)/C(2) bond.[31] An asymmetric allylic amination could be exploited to close the C-ring and set the absolute configuration of the resulting azepine **56** (Figure 7). Sequential Suzuki-Miyaura cross coupling reactions were implemented to obtain the functionalized nitrobenzene **57** in a convergent manner from 2-iodo-3-nitrophenol **58** and vinylboranes **59** and **60**.

Formation of the cyclisation precursor **57** began with protection of 2-iodo-3-nitrophenol **58** as the SEM ether (Scheme 4). Suzuki-Miyaura cross coupling to vinylborane **60** delivered the protected alcohol **61**. DDQ-mediated PMB deprotection followed by a Mitsunobu reaction with BocNHTs delivered the differentially bis-protected primary amine **62**. Treatment of **62** with concentrated HCl led to a deprotection of the acid-labile SEM group, and the resulting phenol **63** was converted to the triflate. A second Suzuki-Miyaura cross-coupling reaction with vinylborane **59** formed diene **64**, and a DDQ-mediated PMB cleavage unmasked the allylic alcohol **65**, which was converted into the key carbonate **57** by reaction with methyl chloroformate followed by Boc deprotection. The prochiral allylic carbonate **57** underwent the intramolecular asymmetric amination reaction in the presence of a catalytic amount of $Pd_2(dba)_3$, the sterically demanding *t*Bu-PHOX ligand **66**, and Bu_4NCl to afford the enantiomerically enriched azepine **56** in 77% yield and 95% ee. The absolute configuration was assigned as (*R*) by analogy to related literature results using ligand **66**.[32]

The isobutenyl side chain was introduced by a cross metathesis using Grubbs' II catalyst and the resulting product was subjected to $P(OEt)_3$ mediated indole formation. Conversion of the azepinoindole **67** to aurantioclavine (**2**) was achieved *via* sequential hydrolysis/ decarboxylation and tosyl cleavage. The natural product was obtained in 16 steps and 11% yield in the longest linear sequence.

3.1.5 Enantioselective total syntheses of (−)-and (+)-aurantioclavine by asymmetric allylic amination—Yang's enantioselective total synthesis of both the natural and the unnatural enantiomer of aurantioclavine serves to further highlight the utility of metal-catalysed asymmetric allylic amination reactions to drive enantioselective synthesis.[33] Yang dissected aurantioclavine in a similar manner to Takemoto by exploiting a late-stage asymmetric amination reaction for the enantioselective annulation of the azepinoindole ring **69** from pre-functionalized 3,4-disubstituted indole intermediate **70** (Figure 8). The requisite allylic alcohol **70** could be obtained from the 4-bromotryptamine derivative **72** by sequential formylation and Grignard addition reactions.

The key asymmetric amination precursor **70** was rapidly accessed from bis-Boc protected 4-bromo-tryptamine **72** in a two step sequence involving formylation with *n*-BuLi and DMF, followed by the addition of vinylmagnesium bromide to the intermediate aldehyde **71** (Scheme 5). With the azepine precursor **70** in hand, the asymmetric allylic amination reaction was explored using $[\{Ir(cod)Cl\}_2]$ and phosphoramidite ligand **73**. Prior work by Carreira's group demonstrated that the choice of acidic promoter and solvent was crucial.[34,35] A Lewis acid screen led to the identification of scandium triflate as the superior acidic promoter and 1,2-dichloroethane as a suitable solvent for clean conversion to the desired aminocyclisation product **74** in 86% yield and 93% ee. Notably, the unnatural enantiomer could also be accessed in 91% yield and 97% ee using *ent*-(**73**). Completion of the synthesis required installation of the isobutenyl group and global Boc deprotection. Unfortunately, all attempts to install the isobutenyl group by cross metathesis either failed, or, at best, led to low isolated yields of the desired product. An alternative approach was then explored whereby the terminal olefin **74** was subjected to dihydroxylation followed by $NaIO_4$-mediated oxidative cleavage of the diol to the corresponding aldehyde. A Julia-Kocienski olefination using tetrazoyl sulfone **75** converted the aldehyde into the requisite isobutenyl group **69**, and subsequent bis-Boc deprotection delivered aurantioclavine (**2**) in 8 steps and 15% overall yield from indole **72**.

3.2 Clavicipitic acid

Clavicipitic acid (**1**) was isolated as a mixture of naturally occurring *cis*- (**1b**) and *trans*- (**1a**) diastereomers from *Claviceps* strain SD-58 and *Claviceps fusiformis* fungi.[36,37] This clavine alkaloid is structurally characterized by the presence of the same azepinoindole core as in aurantioclavine (**2**). In 2010, Jia *et al.* established that the relative configurations of *cis*- (**1b**) and *trans*- (**1a**) clavicipitic acid were incorrectly assigned in the literature and noted that their assignment in past literature should in fact be reversed.[38] This section will briefly highlight two distinct approaches to synthesize enantiomerically pure clavicipitic acid (**1**), which has recently been the subject of a comprehensive review.[39] As with aurantioclavine, a central challenge for any synthesis of clavicipitic acid is the formation of the seven-

membered ring, and this is reflected in the focus on strategies for the diastereoselective annulation of the azepine.

3.2.1 Enantioselective total synthesis of (−)-*trans* and (−)-*cis* clavicipitic acid by Heck coupling/aminocyclisation—A biomimetic total synthesis of enantioenriched *trans*- (**1a**) and *cis*- (**1b**) clavicipitic acid by Murakami's group featured a Heck coupling/aminocyclisation sequence to form the azepine ring. This assembly of the seven-membered ring was first implemented by the Hegedus group in their 1987 synthesis of *N*-acetyl clavicipitic acid methyl ester and has been utilized in several subsequent syntheses.[38,40.41,42,43] Disconnection of the azepine via the N(6)/C(7)-bond simplified the clavicipitic acid scaffold to the 3,4-disubstituted vinyl indole **76** which should be readily accessible through a Heck coupling of 4-bromoindole **77** (Figure 9). The absolute configuration of the amino stereocenter could be established through a kinetic resolution of racemic precursor **78**, which in turn could be rapidly generated from 4-bromoindole (**79**) using an established protocol.[44]

Brominated acetyltryptophan **78** was formed by the reaction of *DL*-serine with 4-bromoindole (**79**) under acidic conditions (Scheme 6). The newly established *N*-acetylamide could be conveniently exploited in an enzymatic kinetic resolution mediated by *Aspergillus acylase*. Selective hydrolysis of the *N*-acetyl group delivered the enantioenriched amino acid **77** in 49% yield and >99% ee. With **77** in hand, the only remaining challenge was the key Heck reaction and S_N2'-aminocyclisation. After extensive experimentation, a one-pot protocol was established. The Heck coupling between tryptophan derivative **77** and 2-methyl-3-buten-2-ol proceeded upon treatment with $Pd(OAc)_2$, in the presence of TPPTS (tris(3-sulfophenyl)phosphine trisodium salt) and K_2CO_3 to deliver the 3,4-disubstituted indole **76**. Direct acidification of the crude Heck reaction mixture with 60% AcOH (aq) at 60 °C triggered the aminocyclisation to provide a mixture of clavicipitic acids in a combined yield of 61%. Notably, no racemization of the stereogenic C(5) was reported despite the harsh basic conditions employed in the Heck reaction. Clavicipitic acid was thereby obtained in 3 steps and 21% yield for the longest linear sequence.

3.2.2 Synthesis of (−)-*cis* clavicipitic acid by reductive amination—Shibata's 2015 synthesis of (−)-*cis* clavicipitic acid (**1b**) features a novel method to synthesize 4-substituted tryptophan derivatives by an iridium-catalysed C-H activation/cyclodehydration sequence.[45] Shibata's work was based on the expectation that indole **80** could be readily converted into (−)-*cis* clavicipitic acid through an intramolecular reductive amination (Figure 10). The C-H activation/cyclodehydration reaction would be deployed on indole precursor **81**, which in turn could be obtained in a convergent manner from aniline **82** and amino acid **83**.

A chiral pool approach was utilized to set the absolute configuration required for (−)-*cis*-clavicipitic acid from the outset of the synthesis (Scheme 7). Conversion of asparagine (**84**) into chiral α-keto bromide **83** was accomplished via a series of standard functional group manipulations. *N*-Alkylation of aniline **82** with bromide **83** proceeded smoothly to afford diketone **81** in 83% yield. The key indole annulation sequence was then investigated. The authors anticipated that the acrolyl substituent at C(3) of aniline **81** would act as a directing

group to coordinate the iridium catalyst and guide its insertion into the proximal Csp_2H bond at C(2). The resulting organoiridium species **85** is positioned in close proximity to the side chain ketone and should be properly oriented to undergo an intramolecular cyclodehydration reaction to furnish indole **80**. Gratifyingly, heating β-keto aniline **81** with $[Ir(cod)_2]$BARF in the presence of *rac*-BINAP resulted in conversion to the desired indole **80** in 79% yield. The final sequence to form the azepine ring and complete the tricyclic core was initiated with removal of the Cbz-carbamate to deliver the corresponding primary amine. The reductive amination to form the azepine ring required careful tuning of reaction conditions. Ultimately, the use of $NaBH(OAc)_3$ in the presence of triethylamine proved effective and hydride delivery to the convex face furnished the *cis*-diastereomer **86** exclusively. Unfortunately, this sequence led to almost complete erosion of ee in the product **86**, which was formed in only 13% ee. With the methyl ester precursor **86** completed in 10 steps and 12% yield, facile saponification with Jia's protocol provided (−)-*cis*-clavicipitic acid (**1b**).[46]

3.3 Rugulovasine A & B

The rearranged clavine alkaloids rugulovasine A (**11a**) and B (**11b**) were first isolated as a pair of naturally occurring diastereomers from the fungus *Penicillium concavorugulosum*.[17] Their fascinating three-dimensional structures were unambiguously determined seven years after the original isolation paper by X-ray crystallographic analysis of rugulovasine A, revealing a tricyclic 3,4-disubstituted indole core adorned with an atypical butenolide moiety.[47] Interestingly, both rugulovasine A and B were isolated as racemates and shown to interconvert in polar solvents.[48] Their interconversion was proposed to occur via an intramolecular vinylogous Mannich reaction proceeding through 2-alkoxyfuran intermediate **87** (Figure 11).[47] This unusual mechanism for interconversion and the ease of its occurrence indicate that either rugulovasine could be an artefact of the isolation procedure, and the transiently formed achiral 2-alkoxyfuran intermediate **87** could explain why rugulovasines A and B were isolated in racemic form. Three synthetic approaches to the rugulovasines are highlighted in this section.

3.3.1 Intermolecular vinylogous Mannich approach to rugulovasines A & B—

Martin's synthesis of rugulovasines A and B was inspired by their proposed mechanism of interconversion.[49] This strategy hinged on the success of an intermolecular Mannich reaction to form butenolide **88**, which should be well-suited for subsequent annulation to produce rugulovasines A (**11a**) and B (**11b**) (Figure 12). Retrosynthetically, the Mannich disconnection leads to the simplified silyloxyfuran **89** and iminium ion **90.** The latter intermediate can be readily obtained from 4-bromoindole **79** that incorporates the indole AB-ring system present in rugulovasines A (**11a**) and B (**11b**) from the outset.

4-Bromoindole (**79**) was converted into indole **91** by a Mannich-type reaction followed by an elimination-addition reaction of the resulting gramine intermediate with potassium cyanide (Scheme 8). Protection of the free indole as the Boc-carbamate followed by DIBAL-H reduction of the nitrile led to the pivotal Mannich precursor **93**. The key sequence commenced with condensation of the crude aldehyde and benzylmethylamine to generate the activated iminium ion **94**, which underwent an acid-catalysed intermolecular Mannich

reaction with silyloxyfuran **89** to furnish a mixture of diastereomeric adducts **95** in 45% overall yield from nitrile **92**. Having installed the butenolide in a convergent manner, an elegant photo-stimulated $S_{RN}1$ reaction was implemented to form the spirolactone moiety in the natural product.[50] In this protocol, butenolide **95** was treated with liquid ammonia at −33 °C in the presence of potassium *tert*-butoxide to generate the corresponding butenolide enolate *in situ*. Irradiation of this solution generated an electrophilic phenyl radical at the C(4) position of the indole, which underwent a coupling reaction with the butenolide enolate to deliver the spirolactone scaffold of rugulovasines A and B, concomitant with a fortuitous cleavage of the Boc-group. The final benzyl deprotection to **11** led to unexpected difficulties attributed in part to the presence of the free indole NH, which prevented a clean deprotection under standard conditions. This issue was eventually resolved by conversion to the hydrochloride salt. This modification facilitated the hydrogenolysis of the benzyl group in the presence of Pearlman's catalyst to deliver a 1:2 mixture of rugulovasines A (**11 a**) and B (**11b**). The latter compound was thus obtained in 11% overall yield and 8 steps from **79**.

3.3.2 Intramolecular vinylogous Mannich approach to rugulovasines A an B— Martin's second approach relied on an intramolecular variant of the Mannich reaction that his group successfully deployed in their first approach to rugulovasines A and B to convert furan **96** into the natural product **11** (Figure 13).[49] A Stille coupling to form furan **96** leads retrosynthetically to indole **91**, which conveniently intersects their prior pathway.

In the Stille coupling of the 4-bromoindole **91** to furan **97**, addition of base was necessary to avoid significant decomposition of the furan starting material through an unproductive protodestannylation pathway (Scheme 9). The resulting crude indole was immediately subjected to Boc-protection to deliver the protected indole **98** in 94% yield. The key Mannich reaction was then carried out using conditions that were optimized on a model system. Thus, treating nitrile **98** with DIBAL-H followed by the addition of anhydrous silica gel just prior to workup delivered the desired Mannich adduct **100** in 71% yield as a mixture of diastereomers. Unfortunately, mono-methylation of amine **100** was unsuccessful and a longer but ultimately more efficient route was pursued whereby the free amine **100** was subjected to sequential mono-Cbz protection and *N*–methylation to produce a diastereomeric mixture of orthogonally bis-protected amine **101**. Sequential deprotection of the Boc group by treatment with Cs_2CO_3 in MeOH followed by hydrogenolysis of the Cbz group delivered a 2:1 mixture of rugulovasine A (**11a**) and B (**11b**) in 74% yield. Interestingly, the formation of rugulovasine A (**11a**) as the major product in 30% overall yield and 8 steps from **79** in this sequence is in contrast to their first approach, which delivered rugulovasine B (**11b**) as the major isomer.

3.3.3 Total synthesis of rugulovasine A by aryl lithium acylation—Jia's total synthesis of rugulovasine A features an intramolecular nucleophilic addition of an aryllithium species to an ester to close the C-ring and highlights two different strategies for late stage butenolide formation.[51] Retrosynthetically, it was expected that the butenolide ring could be accessed from Uhle's ketone derivative **103** by an Nozaki-Hiyama-Kishi (NHK) reaction to form allenic alcohol **102** followed by cyclocarbonylation (Figure 14). The

tricyclic core would be formed from 4-iodoindole **104** through a nucleophilic ring closure initiated by a lithium-halogen exchange.

The 4-iodotrytophan derivative **104** was prepared according to a previously published route (Scheme 10).[38,52] Metal-halogen exchange proceeded smoothly and the resulting carbanion underwent an intramolecular addition reaction to the pendant ester to afford ketone **103** in 80% yield. Unfortunately, the strongly basic conditions required to promote cyclisation led to racemisation of **103**. However, no efforts were made to suppress this process as rugulovasine A had also been isolated in racemic form. The final stages of the synthesis required an elaboration of the spirocyclic butenolide moiety from the tricyclic precursor **103**. This was initially achieved using an annulation strategy initiated by an NHK reaction with propargyl bromide under Goré's conditions to deliver allenic alcohol **102** in 41% yield (or 66% brsm).[53] Compound **102** was isolated as a single diastereomer stemming from addition of the organochromium species to the less-hindered face of the ketone to generate the *cis*-amino alcohol. Allenic alcohol **102** was then transformed into butenolide **105** by a cyclocarbonylation reaction. Unfortunately, attempts to effect a global Boc deprotection led to decomposition. However, a stepwise strategy proved feasible whereby the indole nitrogen was selectively deprotected in 75% yield using Cs_2CO_3 in THF/MeOH. The remaining Boc group was then cleaved with TMSOTf in the presence of 2,6-lutidine to deliver rugulovasine A (**11a**) in an overall yield of 12% and 5 steps from the advanced intermediate **104**.

An alternative and ultimately higher-yielding 2nd generation synthesis to install the butenolide moiety in rugulovasine A was also explored by this group. Reformatsky reaction between Uhle's ketone **103** and methyl 2-(bromomethyl)acrylate delivered lactone **106** as a single diastereomer (Scheme 11). The isomerization of the exocyclic olefin into the butenolide ring proved extremely challenging. Only conditions reported by Takahashi for the isomerization of related lactones were effective at promoting olefin migration to the endocyclic position while heating lactone **106** in dioxane at 100 °C in the presence of $Ru_3(CO)_{12}$ and Et_3N.[54] The desired butenolide **105** was obtained in 95% yield, intersecting their first approach and increasing the overall yield to 45%.

3.4 Cycloclavine

Cycloclavine (**26**) was first isolated in 1969 by Hofmann *et al.* who obtained the alkaloid from seeds of the African morning glory shrub *Ipomea hildebrandtii*.[55] Since its initial discovery, cycloclavine has also been isolated from *Aspergillus japonicus*, a species of filamentous fungi.[56] The absolute configuration of the natural product was unambiguously determined by X-ray analysis of its methobromide salt. From a synthetic perspective, the compact pentacyclic scaffold offers a number of structural challenges. The 3,4-disubstituted indole core is fused to a densely functionalized *trans*-hydroindoline that contains three contiguous stereocenters, two of which are all-carbon quaternary centers and fused into a cyclopropane ring. Cycloclavine has attracted considerable attention in recent years, culminating in several formal and total syntheses. This section summarizes five synthetic paths to this unique ergot alkaloid.

3.4.1 Total synthesis of cycloclavine from Uhle's ketone—Szántay and coworkers published the first total synthesis of racemic cycloclavine (**26**) in 2008.[57] Their approach featured a late-stage installation of the cyclopropane through a Simmons-Smith reaction of the tetrasubstituted olefin **107** (Figure 15). The authors anticipated that cyclisation of the D-ring to form dihydropyrrole **107** could achieved from brominated Uhle's ketone **108** by *N*-alkylation followed by cyclisation.

The key tricyclic intermediate **108** was prepared from readily available 3-indolepropionic acid (**109**) using a previously published route. Annulation of the D ring was achieved through a two-step sequence involving alkylation of ketone **108** with 3-methylaminopropanoate **110** followed by LHMDS-mediated ring closure (Scheme 12). The resulting tertiary alcohol **111** was treated with $POCl_3$ in pyridine followed by HCl in EtOH to deliver the α,β-unsaturated ester **112** as the hydrochloride salt. Reduction of **112** to install the requisite methyl group was achieved with $LiAlH_4$ to give allylic alcohol **113** followed by deoxygenation by sequential treatment with SO_3•Py and $LiAlH_4$. Palladium acetate mediated cyclopropanation of olefin **107** with diazomethane delivered (±)-cycloclavine (**26**) in modest yield. Overall, the synthesis of the pentacyclic ergot alkaloid required 7 steps and proceeded in 1% (brsm) yield from Uhle's ketone derivative **108**.

3.4.2 Total synthesis of cycloclavine by sequential double Diels-Alder reactions—In 2011, Wipf and Petronijevic accomplished a total synthesis of (±)-cycloclavine in 14 steps and 1.2 % overall yield using a strategically distinct consecutive Diels-Alder approach (Figure 16). The cyclopropane was in set in place from the outset of the synthesis, and the indole was formed by an intramolecular Diels-Alder furan (IMDAF) cycloaddition late in the synthetic sequence unlike other syntheses.[58,59,60] Furthermore, a novel intramolecular methylenecyclopropane Diels-Alder reaction was exploited to establish the hydroindoline ring system **114**. The diene precursor **115** could be obtained in a convergent manner via *N*-alkylation of vinylogous amide **117** with mesylate **116**.

THP-protection of β followed by cyclopropanation with dibromocarbene led to *gem*-dibromocyclopropane **119** (Scheme 13). Metal-halogen exchange afforded the corresponding mono-lithiated cyclopropane, which was quenched with MeI. *t*-BuOK was used for the dehydrobromination, and subsequent acid-mediated THP cleavage furnished methylenecyclopropane **120** in good yield. Alcohol **120** was then converted to the corresponding mesylate and coupled with the anion of vinylogous amide **117** to furnish the diene precursor. Enolisation occurred smoothly in the presence of NaHMDS, and the resulting enolate was trapped *in situ* with TBSCl to deliver TBS enol ether **121**. Gratifyingly, the key diene **121** underwent a highly diastereoselective methylenecyclopropane Diels-Alder cycloaddition when subjected to microwave irradiation at 195 °C for 1 h, forming the *endo*-adduct exclusively. Removal of the TBS group was effected with TBAF to form ketone **114**. With the requisite hydroindoline in hand, attention turned to installation of the 3,4-disubstituted-indole core. Oxidation of tricyclic ketone **114** to the corresponding enone failed under standard conditions. This was attributed to the presence of the basic tertiary amine and solved by a dealkylative protection of the amine as the carbamate, which allowed for a Saegusa-Ito oxidation to introduce the requisite olefin and deliver enone **122**. Tin-

lithium exchange of stannane **123** led to the corresponding organolithium reagent, which added to enone **122** in a 1,2-fashion. The resulting tertiary alcohol **124** was subjected to a microwave promoted IMDAF reaction to give Diels-Alder adduct **125**, which underwent a cascade double dehydrative aromatization to furnish indole **126** in 44% yield. Finally, LAH reduction of carbamate **126** afforded cycloclavine in quantitative yield.

3.4.3 Formal & total synthesis of cycloclavine by fragmentation and 1,3-dipolar cycloaddition—Brewer's strategy featured a late stage D-ring annulation, which relies upon an elegant fragmentation/cycloaddition sequence for the conversion of diazo acetate **129** into dihydropyrrole **127** *via* aldehyde ynoate intermediate **128** (Figure 17).[61] The group anticipated that the fragmentation precursor **129** could be obtained from pivaloated Uhle's ketone **130** in which the A-, B-, and C-rings of cycloclavine are already preformed.

Rubottom oxidation of the protected ketone **130** yielded an intermediate α-hydroxy ketone, which was trapped as the TBS ether **131** (Scheme 14). Aldol-type addition of ethyl lithiodiazoacetate to ketone **131** delivered the crucial γ-siloxy-β-hydroxy-α-diazo ester **129** as an inseparable mixture of diastereomers. The key fragmentation reaction proceeded smoothly upon the addition of $SnCl_4$ to deliver tethered aldehyde ynoate **128.** Treatment of **128** with sarcosine silyl ester **133** generated azomethine ylide **134** that underwent an intramolecular 1,3-dipolar cycloaddition to give the expected 2,5-dihydropyrrole in 65% yield. Upon pivaloate deprotection to indole **112**, the route intercepted Szántzay's synthesis. Furthermore, in order to investigate alternative cyclopropanation conditions, indole **112** was tosylated and subjected to a variety of reaction conditions. Unfortunately the tetrasubstituted olefin proved unreactive toward diazomethane cyclopropanation and the Corey-Chaykovsky procedure. The ester was then reduced to the corresponding allylic alcohol **135** and subjected to Simmons-Smith type reagents. Attempts to effect cyclopropanation of olefin **135** with Zn, Sm, Pd, Mg and Cr failed, and only Charette's *gem*-dizinc carbenoid conditions provided the desired cyclopropane **136**, albeit in low yield. The synthesis was completed by deoxygenation *via* mesylation/hydride displacement of primary alcohol **136** and hydrolysis of the sulfonamide. This approach provided the racemic natural product in 13 steps and 1.1% overall yield from tricycle **130**.

3.4.4 Formal synthesis of cycloclavine by aza-Cope Mannich/radical cyclisation—Cao et al. reported a concise formal synthesis of cycloclavine based on a late stage construction of the CD-ring system.[62] The group planned to close the C-ring through either a Heck-type coupling or a radical cyclisation of functionalized pyrrolidine **137**, which in turn could be accessed through a key tandem aza-Cope Mannich reaction of 3,4-disubstituted indole **139** and 2-hydroxy homopropargyl tosylamine (**138**) (Figure 18).[63]

The known aldehyde **139** was prepared in 4 steps and 72% overall yield from 4-bromoindole **79** (Scheme 15). Upon exposure of aldehyde **139** to 2-hydroxy homopropargylamine (**138**) in the presence of $FeCl_3$, a condensation reaction delivered iminium ion **140**, which underwent a spontaneous aza-Cope reaction to form ketene **141**. The subsequent intramolecular Mannich reaction provided pyrrolidine **137** in 83% yield. Next, focus shifted to the construction of the C-ring. Attempts to use a Heck coupling for ring closure proved

low yielding, but an alternative radical-initiated ring closure pathway was more successful. Aldehyde **137** was reduced to the corresponding alcohol and treated with diphenyl disulfide and tri-*n*-butylphosphine to deliver sulfide **142** in 81% yield. Treatment of **142** with tributyltin hydride/AIBN prompted a 6-*exo*-*trig* aryl radical-alkene cyclisation to tetracycle **143**. Isomerization of the olefin **143** to the tetrasubstituted olefin **144** was effected with *p*-TsOH•H_2O in refluxing benzene. Szántzay's intermediate **107** was then accessed by sodium naphthalenide-mediated cleavage of the tosyl groups and subsequent *N*-methylation, completing the formal synthesis of cycloclavine in 27% yield and 7 steps from known aldehyde **139**.

3.4.5 Formal synthesis of cycloclavine by Heck coupling—In 2016, the Opatz group reported another convergent approach to the tetracyclic portion of the cycloclavine core.[64] Their strategy was guided by the expectation that the C-ring could be established late in the synthetic sequence through the union of an appropriately functionalized D-ring scaffold with an indole derivative, which comprises the AB-ring system of the natural product (Figure 19). Consecutive enolate alkylation and Heck-coupling of pyrrolinone **146** and indole **147** was expected to afford the key tetracycle **145**. A series of functional group manipulations on **145** would then be carried out to deliver (±)-cycloclavine.

The synthesis of the D-ring fragment began with mono-methylation of allylamine (**148**) through a two-step sequence involving formylation followed by $LiAlH_4$ reduction (Scheme 16). *N*-Allylmethylamine (**149**) was then coupled with methacryloyl chloride **150** to deliver the corresponding amide **151**. Crude **151** was immediately subjected to a ring closing metathesis reaction in the presence of catMETium catalyst **152** to deliver the pyrrolinone **146** in 73% yield.[65]

The synthesis of the AB-ring fragment was achieved in four steps affording the bis-bromoindole derivative **147** in 78% overall yield. The crucial coupling reaction was initiated by deprotonation of pyrrolinone **146** with NaH to form the corresponding anion **153**, which added to bis-bromoindole **147** in 52% yield to form the desired γ-substituted **154**. The high regioselectivity observed for addition at the γ-position of anion **153** rather than the α-position was attributed to the steric demand imposed by the bulky bromine substituent in the S_N2 transition state. An intramolecular Heck coupling in the presence of Ag_2CO_3 proceeded cleanly to furnish tetracycle **145** in 74% yield. Reduction of the lactam with $LiAlH_4$ was accompanied by Boc-cleavage to deliver amine **107**, which intercepted Szántay's route and, thus completed another formal synthesis of cycloclavine in 17% yield and 7 steps for the longest linear sequence.

4. Biological Profile

Both clavine and lysergic acid alkaloids display an extraordinarily broad spectrum of biological activity, spanning multiple therapeutic areas including infectious diseases, CNS disorders, obstetrics and oncology.[1] These alkaloids bear a strong structural resemblance to the natural neurotransmitters serotonin, dopamine and adrenalin, so it is not surprising that this diverse pharmacological profile is often attributed to their ability to mimic or block the binding of these neurotransmitters to their receptors. While the biological activity of lysergic

acid-type alkaloids has long been exploited for drug development by the pharmaceutical industry, the therapeutic potential of clavines still remains largely unexplored despite their medicinally relevant activities. A number of natural clavines exhibit promising anti-cancer properties. For example, fumigaclavine C (**24**) shows cytotoxicity in mouse leukemia P388 and human MCF-7 breast cancer cell lines, and its derivative 9-deacetoxyfumigaclavine C (**155**) displayed selective cytotoxicity in the human leukemia cell line K562 with an IC_{50} of 3.1 μM (Figure 20).[66,67,68] Pibosin B (**156**) proved cytotoxic in mouse Ehrlich carcinoma cells with an ED_{50} of 25 μg/mL, and agroclavine exhibited cytotoxicity against a mouse lymphoma cell line L5178y.[69,70] Chlororugulovasine B (**157**) was acutely toxic to day-old cockerels with an LD_{50} of approximately 75–125 mg/kg.[47,71,72] Several marketed pharmaceuticals as well as drug development candidates are structurally related to clavine alkaloids. For example, pergolide (**158**) is a semi-synthetic clavine alkaloid developed by Eli Lily to treat early-onset Parkinson's disease and has been used clinically to treat more than 1.7 million patients to date.[73] Rucaparib (**159**), which bears strong structural resemblance to the rearranged clavine alkaloids aurantioclavine and clavicipitic acid, is in phase II (NCT02505048) clinical trials for metastatic breast cancer and phase II (NCT01891344) & III (NCT01968213) clinical trials for advanced ovarian cancer.

In addition to their potential and actual use as therapeutic agents, there is considerable interest in clavine alkaloids as novel agrochemicals. Cycloclavine (**26**) and its derivatives have recently emerged as potential insecticides. For example, exposure of cotton, cowpea and green peach aphids to cycloclavine or its methyl carbamate **160** at 300 ppm concentration showed a mortality of 75% compared to untreated controls. The methyl carbamate **160** also showed a mortality of 75% at 300 ppm in diamond black moth, orchid thrips, red spider mite and striped flea beetle. Cycloclavine induced a mortality of 75% at 2,500 ppm in vetch aphid and at 300 ppm in rice green leafhopper and silverleaf whitefly.[74]

Conclusions

The clavines are a structurally and biologically fascinating group of alkaloids whose therapeutic potential remains underexplored. Their structural complexity and novel skeletal connectivity represent a formidable synthetic challenge that has attracted increased attention from academic groups over the past 15 years. A number of innovative total syntheses of clavine alkaloids aurantioclavine, clavicipitic acid, rugulovasines A and B, and cycloclavine have been accomplished, laying the foundation for future medicinal chemistry research. A variety of natural product-related compounds can be envisioned that have the potential to display attractive pharmacological profiles. Increased targeted as well as high-throughput biological testing of clavine chemical library collections would likely pinpoint novel therapeutic applications.

Supplementary Material

Refer to Web version on PubMed Central for supplementary material.

Acknowledgments

The authors gratefully acknowledge funding by the National Science Foundation and the National Institutes for Health in support of alkaloid total synthesis. SRM also gratefully acknowledges funding from the Mary E. Warga and the University of Pittsburgh School of Arts and Sciences Predoctoral Fellowships.

Notes and references

1. Hofmann, A. Plants in the developments of modern medicine. Swain, T., editor. Cambridge, Mass: Harvard University Press; 1972. p. 235-260.
2. Lee MR. J. R. Coll. Physicians Edinb. 2009; 39:179–184. [PubMed: 19847980]
3. Tittlemier SA, Drul D, Roscoe M, McKendry T. J Agric. Food Chem. 2015; 63:6644–6650. [PubMed: 26134095]
4. Coufal-Majewski S, Stanford K, McAllister T, Blakley B, McKinnon J, Chaves AV, Wang Y. Front. Vet. Sci. 2016; 3:15. [PubMed: 26942186]
5. Miedaner T, Geiger HH. Toxins. 2015; 7:659–678. [PubMed: 25723323]
6. Schardl CL, Panaccione DG, Tudzynski P. Alkaloids: Chem. Biol. 2006; 63:45–86. [PubMed: 17133714]
7. Wäli PP, Wäli PR, Saikkonen K, Tuomi J. PLoS ONE. 2013; 8:e69249. [PubMed: 23874924]
8. Wallwey C, Li S-M. Nat. Prod. Rep. 2011; 28:496–510. [PubMed: 21186384]
9. Jakubczyk D, Cheng JZ, O'Connor SE. Nat. Prod. Rep. 2014; 31:1328–1338. [PubMed: 25164781]
10. Young CA, Schardl CL, Panaccione DG, Florea S, Takach JE, Charlton ND, Moore N, Webb JS, Jaromczyk J. Toxins. 2015; 7:1273–1302. [PubMed: 25875294]
11. Jakubczyk D, Caputi L, Hatsch A, Nielsen CAF, Diefenbacher M, Klein J, Molt A, Schröder H, Cheng JZ, Naesby M, O'Connor SE. Angew. Chem. Int. Ed. 2015; 54:5117–5121.
12. Keller NP, Turner G, Bennett JW. Nat. Rev. Microbiol. 2005; 3:937–947. [PubMed: 16322742]
13. Goetz KE, Coyle CM, Cheng JZ, O'Connor SE, Panaccione DG. Curr. Genet. 2011; 57:201–211. [PubMed: 21409592]
14. Lorenz N, Olšovská J, Šulc M, Tudzynski P. Appl. Environ. Microbiol. 2010; 76:1822–1830. [PubMed: 20118373]
15. Robbers JE, Otsuka H, Floss HG, Arnold EV, Clardy J. J Org. Chem. 1980; 45:1117–1121.
16. Lin H-C, Chiou G, Chooi Y-H, McMahon TC, Xu W, Garg NK, Tang Y. Angew. Chem. Int. Ed. 2015; 54:3004–3007.
17. Abe M, Ohmomo S, Ōhashi T, Tabuchi T. Agr. Biol. Chem. 1969; 33:469–471.
18. Robinson SL, Panaccione DG. Toxins. 2015; 7:201–218. [PubMed: 25609183]
19. Panaccione DG. FEMS Microbiol. Lett. 2005; 251:9–17. [PubMed: 16112823]
20. Cheng JZ, Coyle CM, Panaccione DG, O'Connor SE. J Am. Chem. Soc. 2010; 132:12835–12837. [PubMed: 20735127]
21. Coyle CM, Cheng JZ, O'Connor SE, Panaccione DG. Appl. Environ. Microbiol. 2010; 76:3898–3903. [PubMed: 20435769]
22. Kozlovskiĭ AG, Solov'eva TF, Sakharovski VG, Adanin VM. Dokl. Akad. Nauk SSSR. 1981; 260:230–233. [PubMed: 7307906]
23. Numata A, Takahashi C, Ito Y, Takada T, Kawai K, Usami Y, Matsumura E, Imachi M, Ito T, Hasegawa T. Tetrahedron Lett. 1993; 34:2355–2358.
24. Krishnan S, Bagdanoff JT, Ebner DC, Ramtohul YK, Tambar UK, Stoltz BM. J Am. Chem. Soc. 2008; 130:13745–13754. [PubMed: 18798630]
25. Behenna DC, Krishnan S, Stoltz BM. Tetrahedron Lett. 2011; 52:2152–2154.
26. Ferreira EM, Stoltz BM. J Am. Chem. Soc. 2001; 123:7725–7726. [PubMed: 11481006]
27. Yamada K, Namerikawa Y, Haruyama T, Miwa Y, Yanada R, Ishikura M. Eur. J. Org. Chem. 2009; 33:5752–5759.
28. Brak K, Ellman JA. Org. Lett. 2010; 12:2004–2007. [PubMed: 20356065]
29. Brak K, Ellman JA. J Org. Chem. 2010; 75:3147–3150. [PubMed: 20387846]

30. Suetsugu S, Nishiguchi H, Tsukano C, Takemoto Y. Org. Lett. 2014; 16:996–999. [PubMed: 24460216]
31. Chatterjee AK, Sanders DP, Grubbs RH. Org. Lett. 2002; 4:1939–1942. [PubMed: 12027652]
32. von Matt P, Loiseleur O, Koch G, Pfaltz A, Lefeber C, Feucht T, Helmchen G. Tetrahedron: Asymmetry. 1994; 5:573–584.
33. Lei T, Zhang H, Yang Y-R. Tetrahedron Lett. 2015; 56:5933–5936.
34. Lafrance M, Roggen M, Carreira EM. Angew. Chem. Int. Ed. 2012; 51:3470–3473.
35. Schafroth MA, Sarlah D, Krautwald S, Carreira EM. J Am. Chem. Soc. 2012; 134:20276–20278. [PubMed: 23193947]
36. Robbers JE, Floss HG. Tetrahedron Lett. 1969; 10:1857–1858. [PubMed: 5794444]
37. King GS, Mantle PG, Szczyrbak CA, Waight ES. Tetrahedron Lett. 1973; 14:215–218.
38. Xu Z, Hu W, Liu Q, Zhang L, Jia Y. J Org. Chem. 2010; 75:7626–7635. [PubMed: 20964278]
39. Ito M, Tahara Y-K, Shibata T. Chem. Eur. J. 2016; 22:5468–5477. [PubMed: 26822254]
40. Yokoyama Y, Hikawa H, Mitsuhashi M, Uyama A, Hiroki Y, Murakami Y. Eur. J. Org. Chem. 2004; 2004:1244–1253.
41. Harrington PJ, Hegedus LS, McDaniel KF. J Am. Chem. Soc. 1987; 109:4335–4338.
42. Yokoyama Y, Matsumoto T, Murakami Y. J Org. Chem. 1995; 60:1486–1487.
43. Ku J-M, Jeong B-S, Jew S-s, Park H-g. J Org. Chem. 2007; 72:8115–8118. [PubMed: 17877402]
44. Snyder HR, MacDonald JA. J Am. Chem. Soc. 1955; 77:1257–1259.
45. Tahara YK, Ito M, Kanyiva KS, Shibata T. Chem. Eur. J. 2015; 21:11340–11343. [PubMed: 26178075]
46. Liu Q, Li Q, Ma Y, Jia Y. Org. Lett. 2013; 15:4528–4531. [PubMed: 23931070]
47. Cole RJ, Kirksey JW, Clardy J, Eickman N, Weinreb SM, Singh P, Kim D. Tetrahedron Lett. 1976; 17:3849–3852.
48. Rebek J, Shue Y-K, Tai DF. J Org. Chem. 1984; 49:3540–3545.
49. Liras S, Lynch CL, Fryer AM, Vu BT, Martin SF. J Am. Chem. Soc. 2001; 123:5918–5924. [PubMed: 11414824]
50. Rossi RA, Bunnett JF. J Org. Chem. 1973; 38:1407–1410.
51. Zhang Y-A, Liu Q, Wang C, Jia Y. Org. Lett. 2013; 15:3662–3665. [PubMed: 23819853]
52. Liu Q, Jia Y. Org. Lett. 2011; 13:4810–4813. [PubMed: 21866948]
53. Place P, Vernière C, Goré J. Tetrahedron. 1981; 37:1359–1367.
54. Yoneda E, Zhang S-W, Zhou D-Y, Onitsuka K, Takahashi S. J Org. Chem. 2003; 68:8571–8576. [PubMed: 14575487]
55. Stauffacher D, Niklaus P, Tscherter H, Weber HP, Hofmann A. Tetrahedron. 1969; 25:5879–5887. [PubMed: 5373534]
56. Furuta T, Koike M, Abe M. Agric. Biol. Chem. 1982; 46:1921–1922.
57. Incze M, Dörnyei G, Moldvai I, Temesvári-Major E, Egyed O, Szántay C. Tetrahedron. 2008; 64:2924–2929.
58. Petronijevic FR, Wipf P. J Am. Chem. Soc. 2011; 133:7704–7707. [PubMed: 21517102]
59. Boonsompat J, Padwa A. J Org. Chem. 2011; 76:2753–2761. [PubMed: 21391623]
60. Petronijevic F, Timmons C, Cuzzupe A, Wipf P. Chem. Commun. 2009:104–106.
61. Jabre ND, Watanabe T, Brewer M. Tetrahedron Lett. 2014; 55:197–199. [PubMed: 24511164]
62. Wang W, Lu J-T, Zhang H-L, Shi Z-F, Wen J, Cao X-P. J Org. Chem. 2014; 79:122–127. [PubMed: 24279324]
63. Overman LE, Kakimoto M-A. J Am. Chem. Soc. 1979; 101:1310–1312.
64. Netz N, Opatz T. J Org. Chem. 2016; 81:1723–1730. [PubMed: 26811951]
65. Jafarpour L, Schanz H-J, Stevens ED, Nolan SP. Organometallics. 1999; 18:5416–5419.
66. Zhang D, Satake M, Fukuzawa S, Sugahara K, Niitsu A, Shirai T, Tachibana K. J Nat. Med. 2012; 66:222–226. [PubMed: 21792727]
67. Li Y-X, Himaya SWA, Dewapriya P, Zhang C, Kim S-K. Mar. Drugs. 2013; 11:5063–5086. [PubMed: 24351905]

68. Ge HM, Yu ZG, Zhang J, Wu JH, Tan RX. J Nat. Prod. 2009; 72:753–755. [PubMed: 19256529]
69. Makarieva TN, Dmitrenok AS, Dmitrenok PS, Grebnev BB, Stonik VA. J Nat. Prod. 2001; 64:1559–1561. [PubMed: 11754612]
70. Eich E, Eichberg D, Müller WEG. Biochem. Pharmacol. 1984; 33:523–526. [PubMed: 6200118]
71. Cole RJ, Kirksey JW, Cutler HG, Wilson DM, Morgan-Jones G. Can. J. Microbiol. 1976; 22:741–744. [PubMed: 1276998]
72. Dorner JW, Cole RJ, Hill R, Wicklow D, Cox R-H. Appl. Environ. Microbiol. 1980; 40:685–687. [PubMed: 7425621]
73. Cabri W, Roletto J, Olmo S, Fonte P, Ghetti P, Songia S, Mapelli E, Alpegiani M, Paissoni P. Org. Process Res. Dev. 2006; 10:198–202.
74. Körber, K., Song, D., Rheinheimer, J., Kaiser, F., Dickhaut, J., Narine, A., Culbertson, DL., Thompson, S., Rieder, J. WO2014096238 A1. 2014.

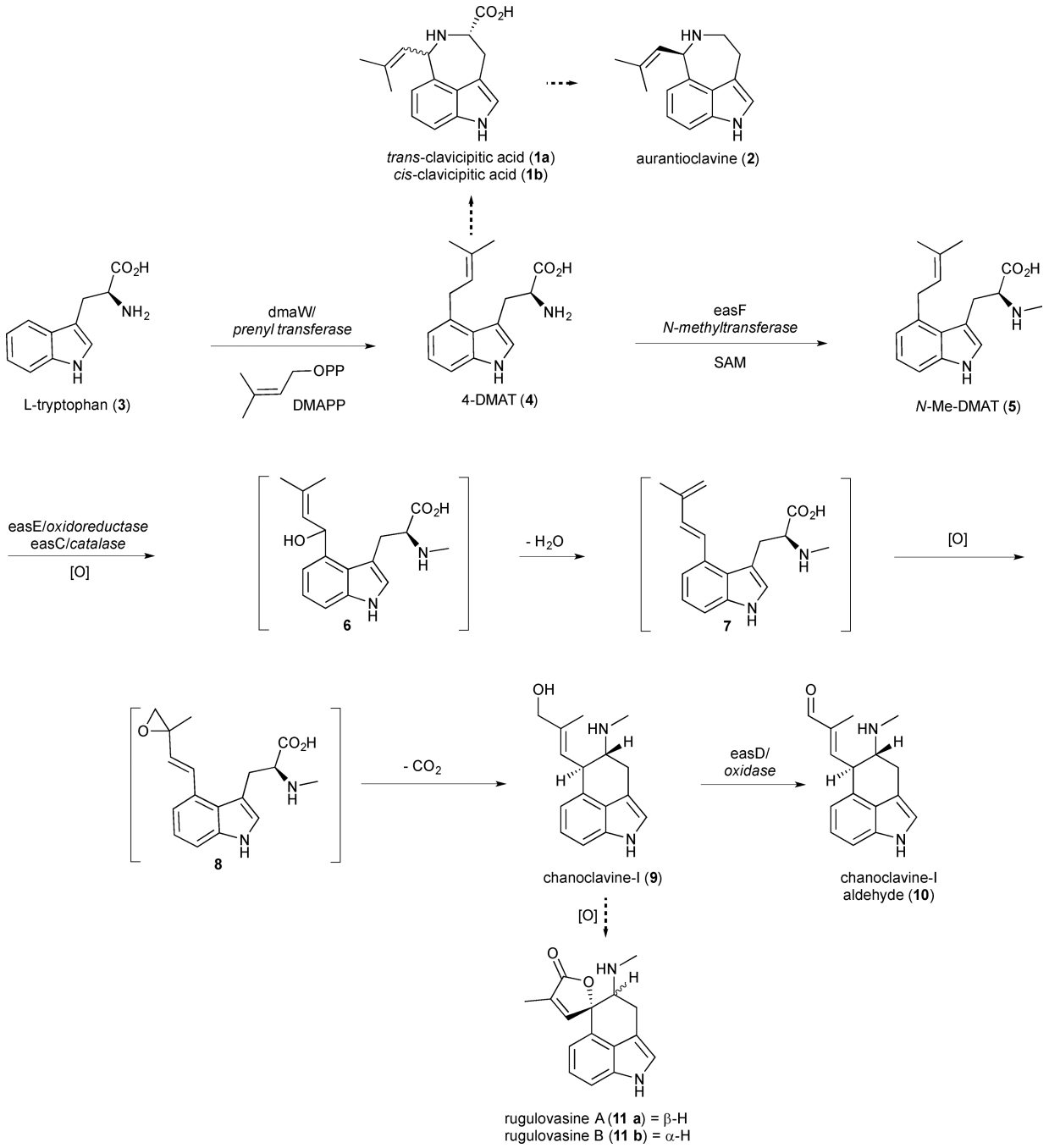

Figure 1.
Early biosynthetic pathway steps and diverted ‘shunt’ products

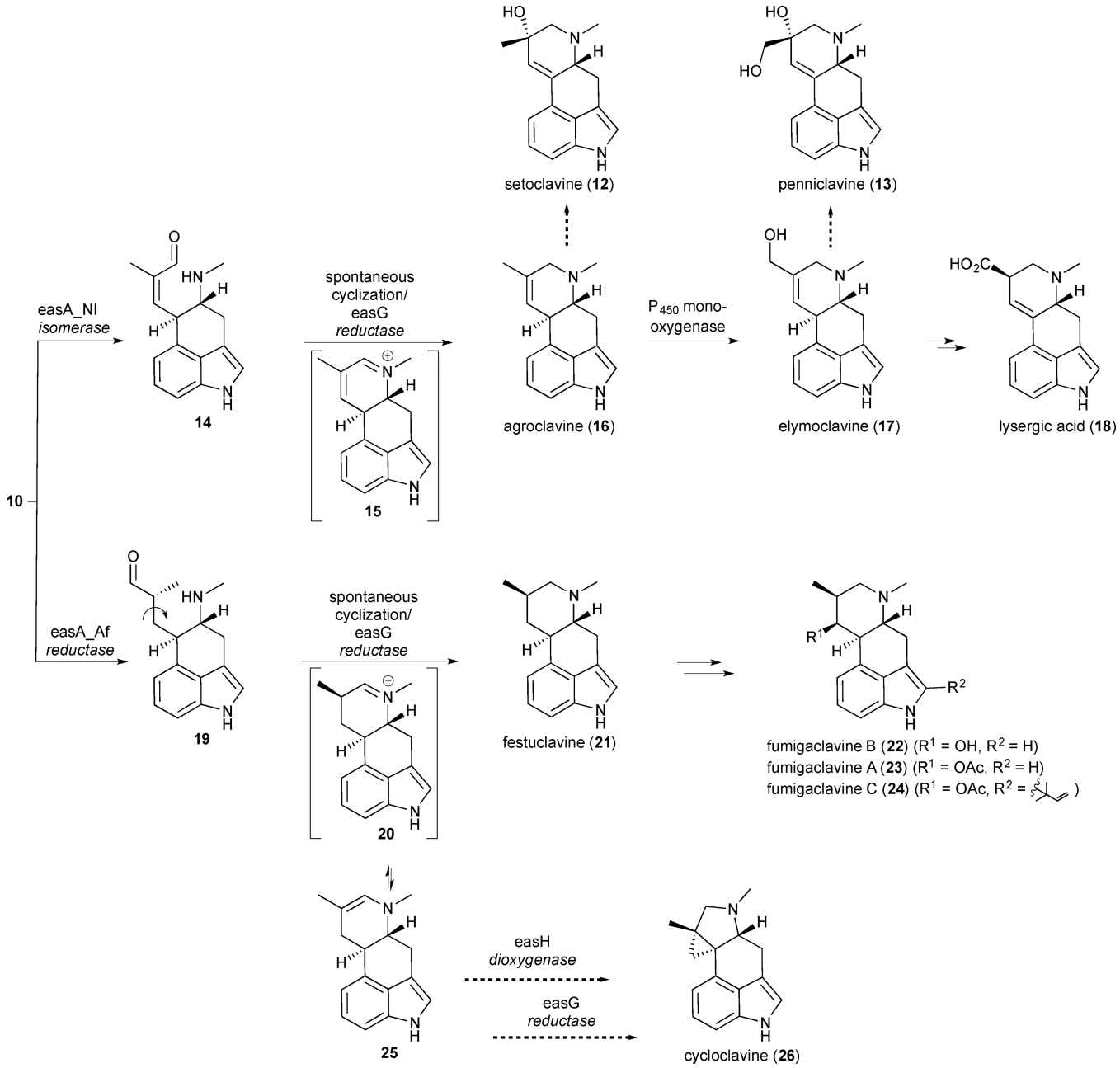

Figure 2.
Late biosynthetic pathway steps and diverted ‘shunt’ pathways

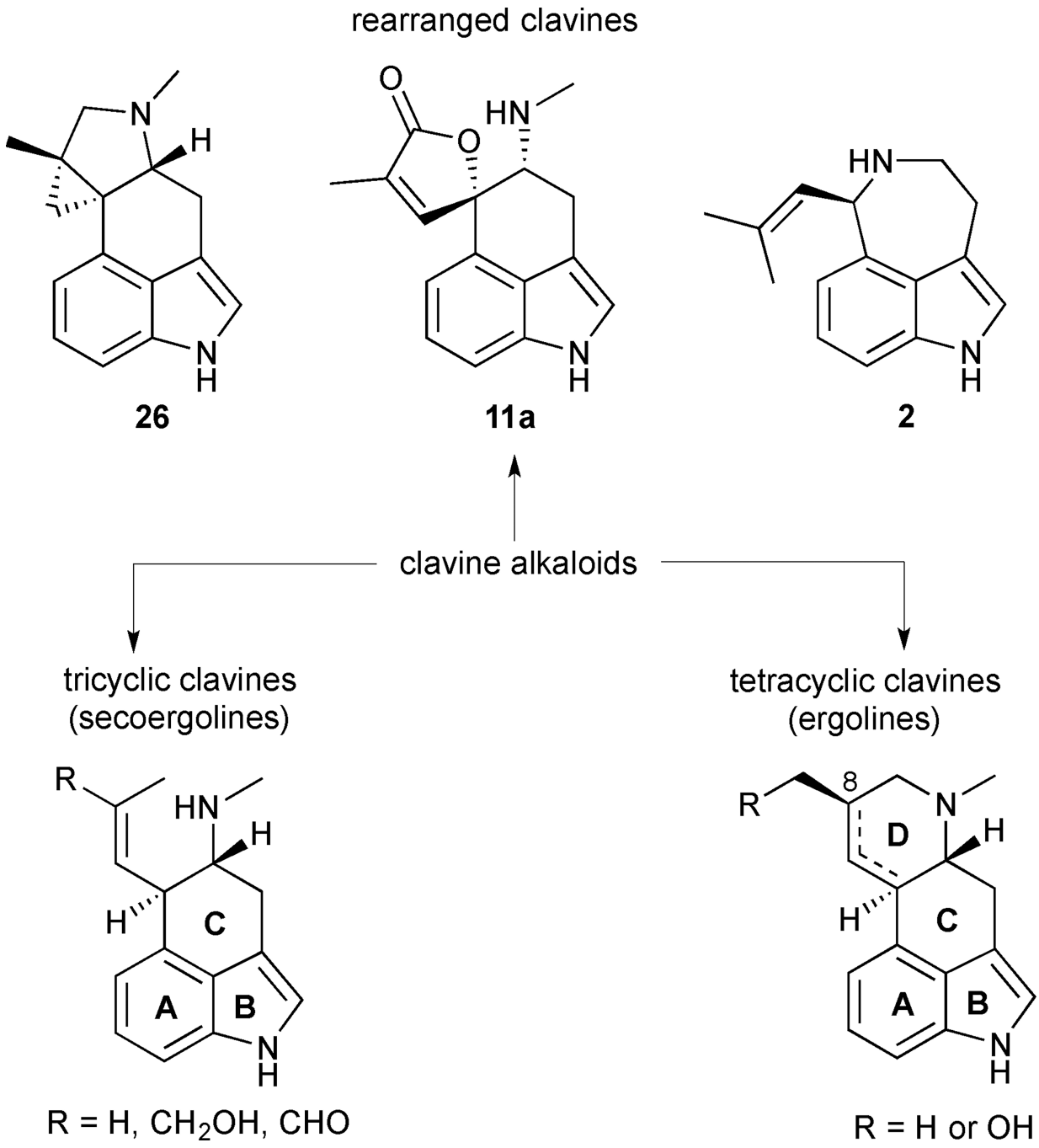

Figure 3.
Classification of tricyclic, tetracyclic and rearranged clavine alkaloids

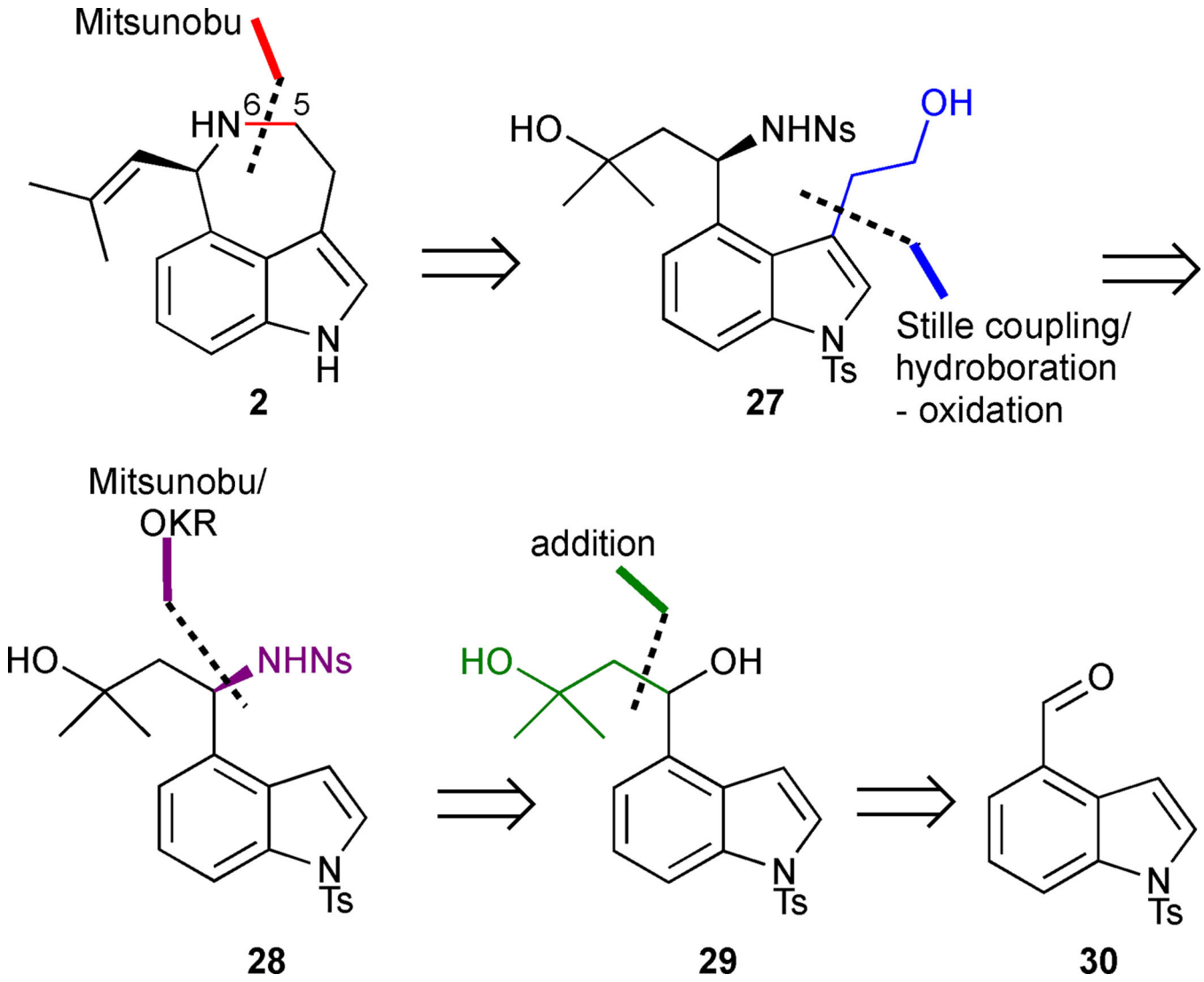

Figure 4.
Retrosynthetic analysis of Stoltz's approach to (−)-aurantioclavine (**2**)

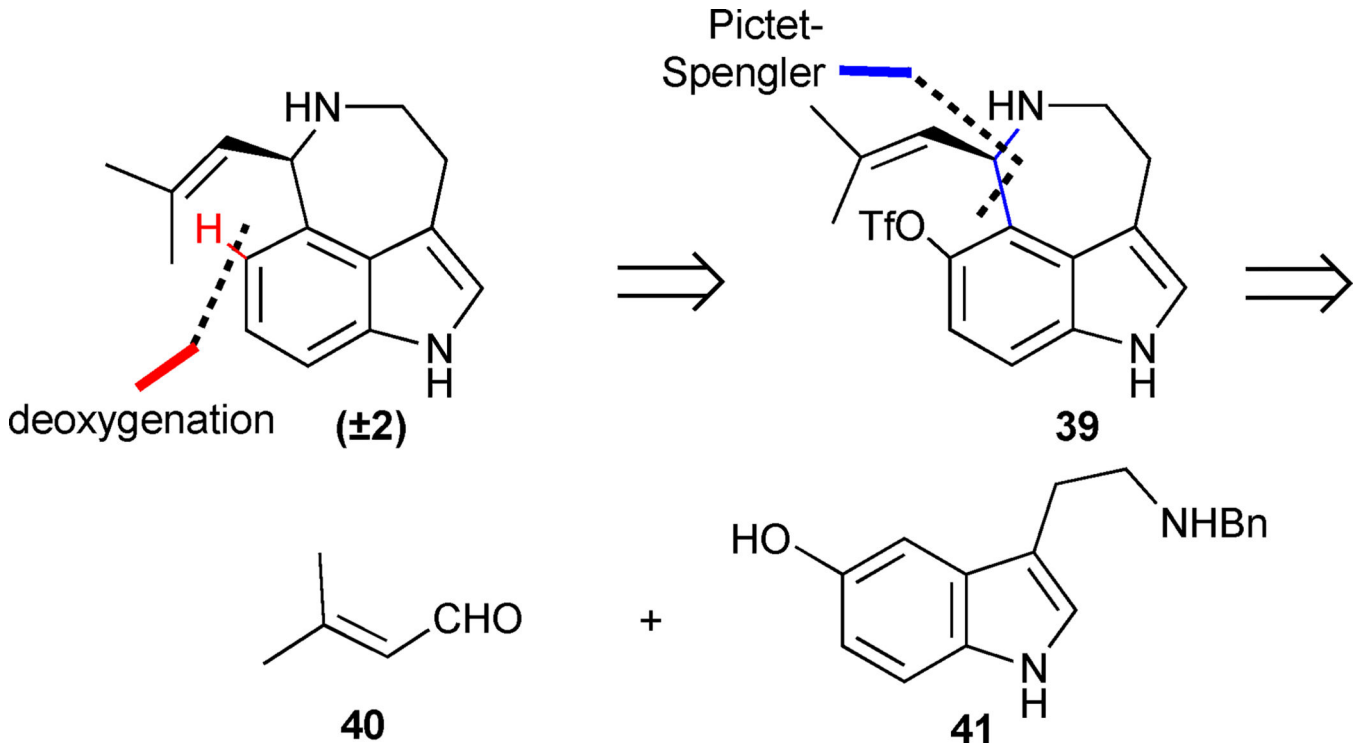

Figure 5.
Retrosynthetic analysis of Ishikura's approach to (±)-aurantioclavine (**2**)

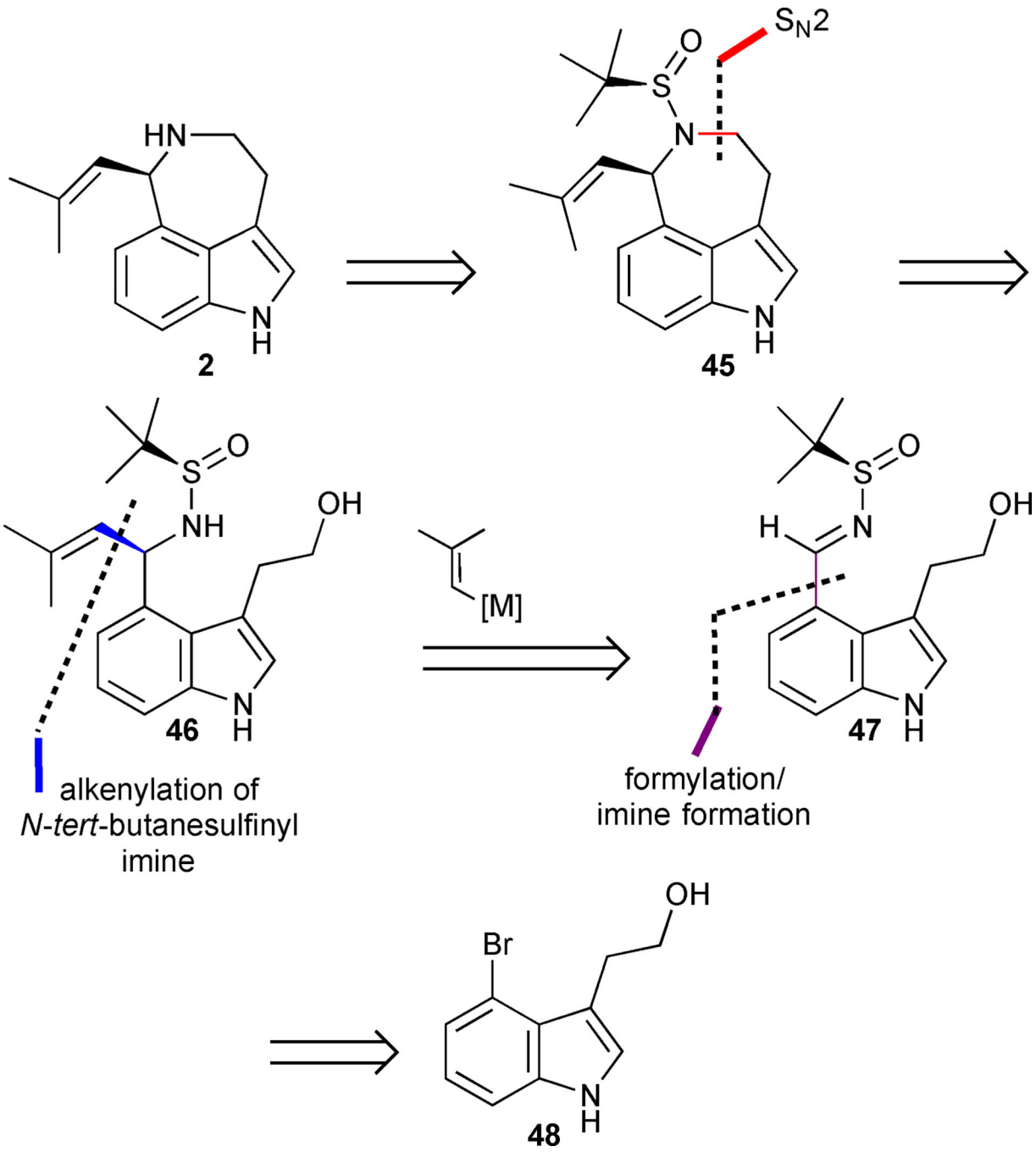

Figure 6.
Retrosynthetic analysis of Ellman's approach to (−)-aurantioclavine (**2**).

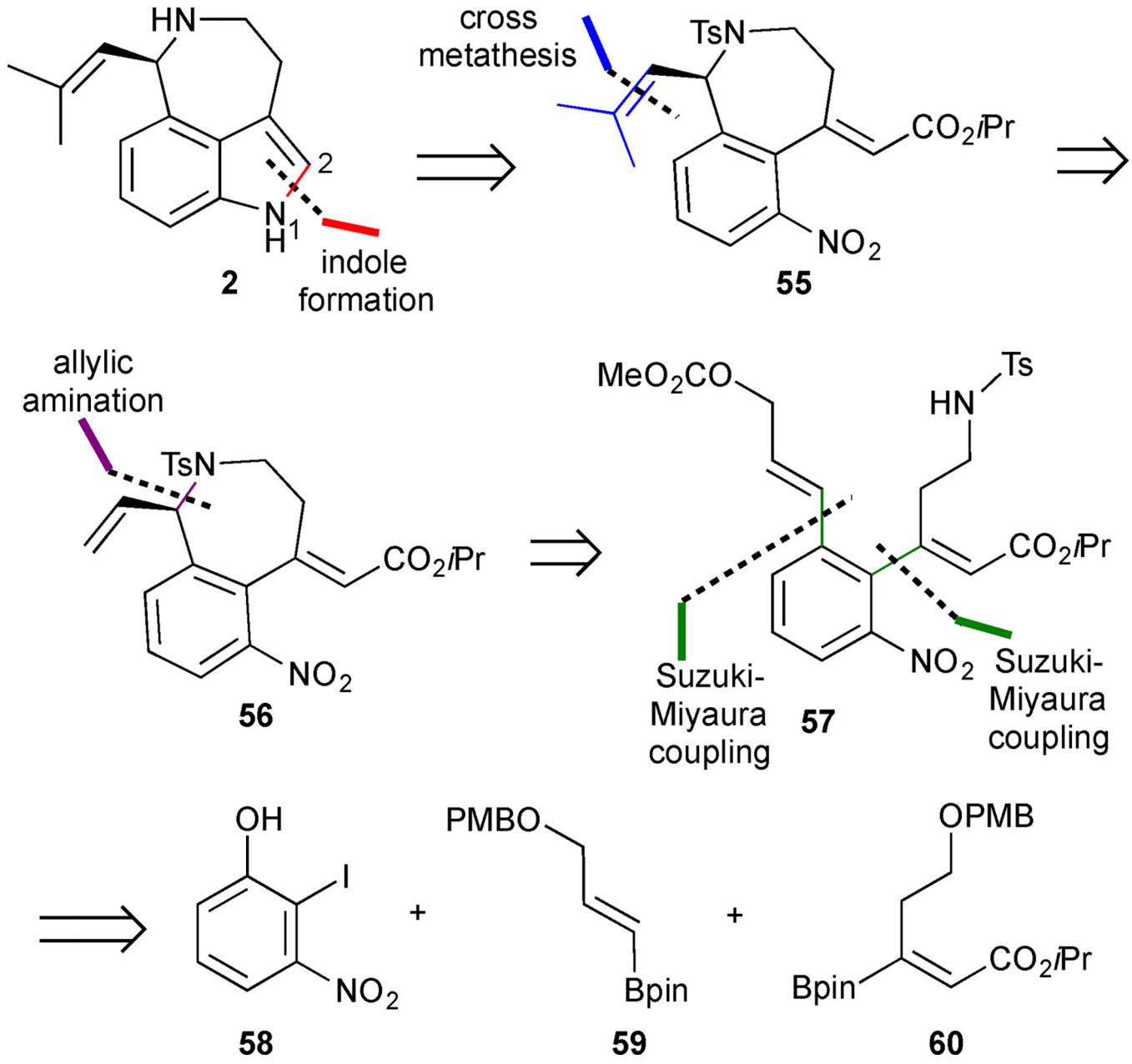

Figure 7.
Retrosynthetic analysis of Takemoto's approach to (−)-aurantioclavine (**2**).

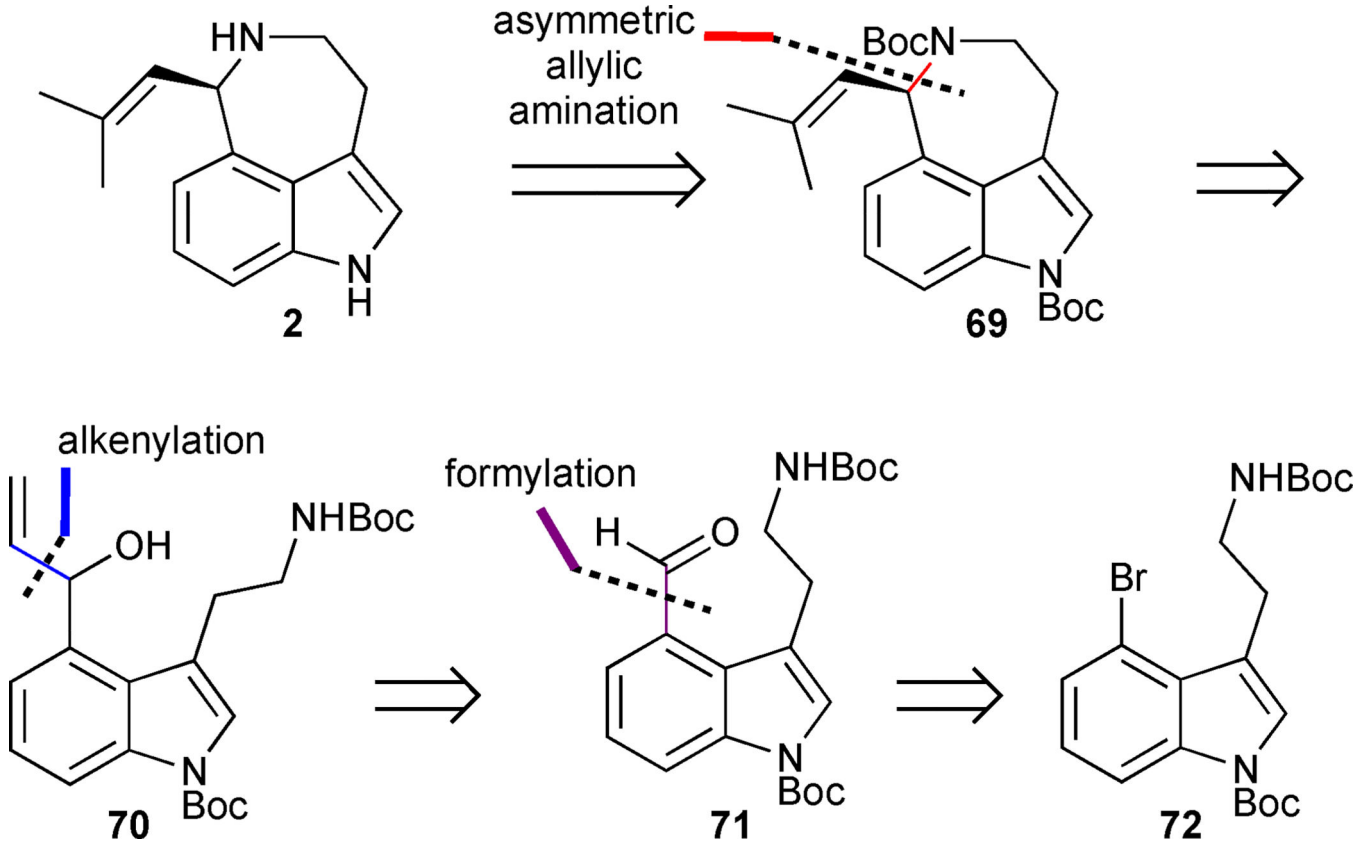

Figure 8.
Retrosynthetic analysis of Yang's approach to (−)-aurantioclavine (**2**).

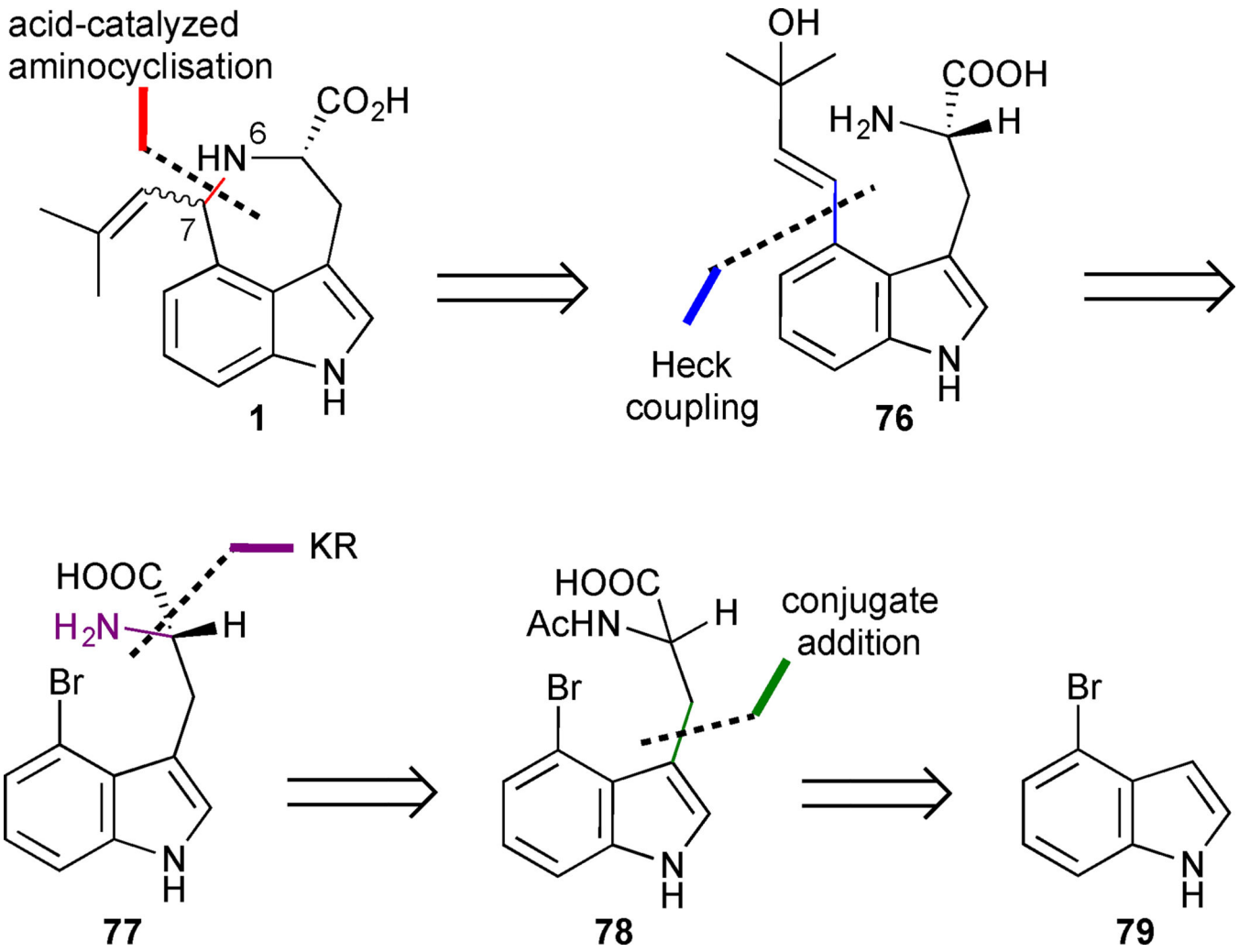

Figure 9.
Retrosynthetic analysis of Murakami's approach to (−)-*cis* and (−)-*trans* clavicipitic acid (**1**).

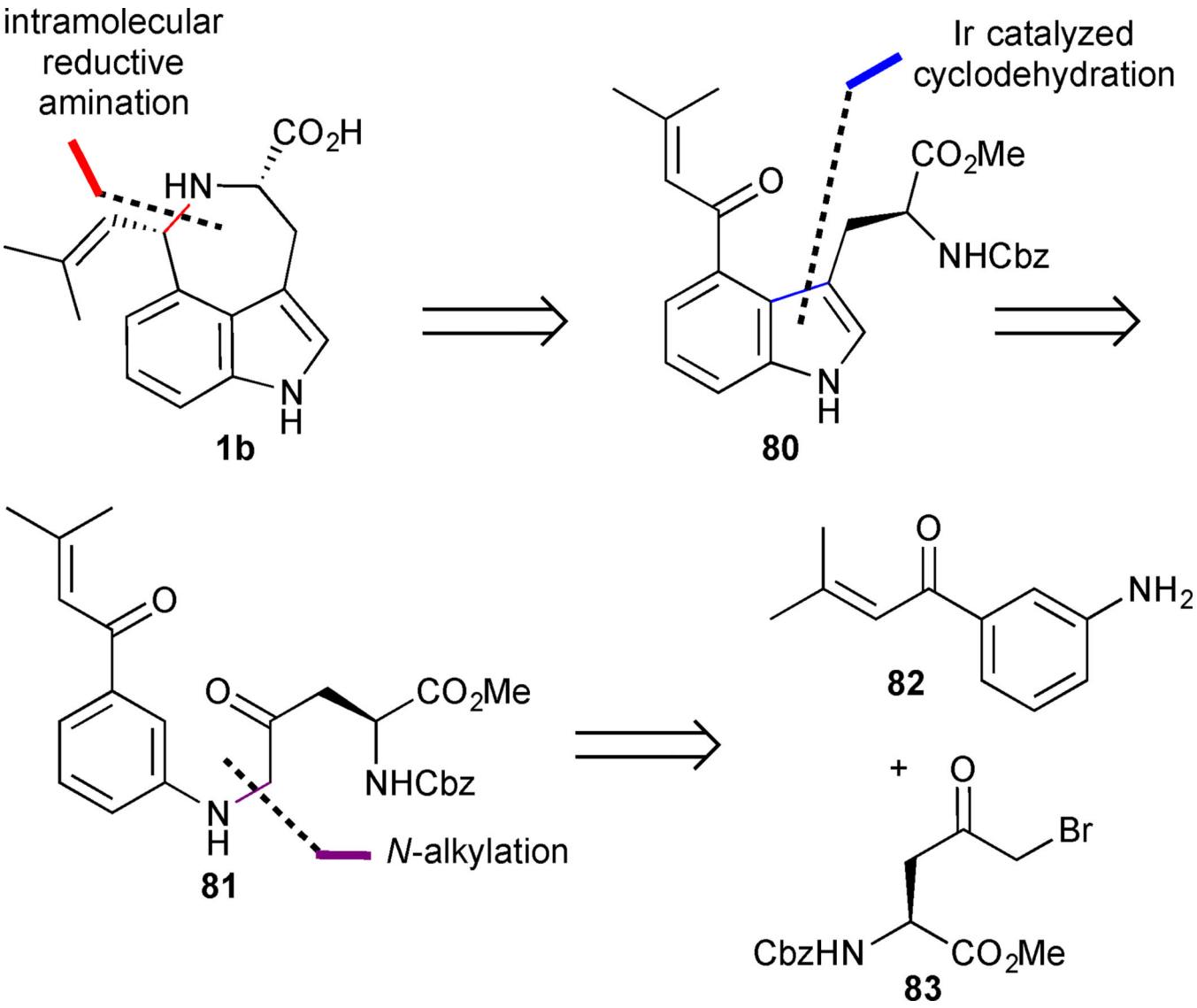

Figure 10.
Retrosynthetic analysis of Shibata's approach to (−)-*cis*-clavicipitic acid (**1b**).

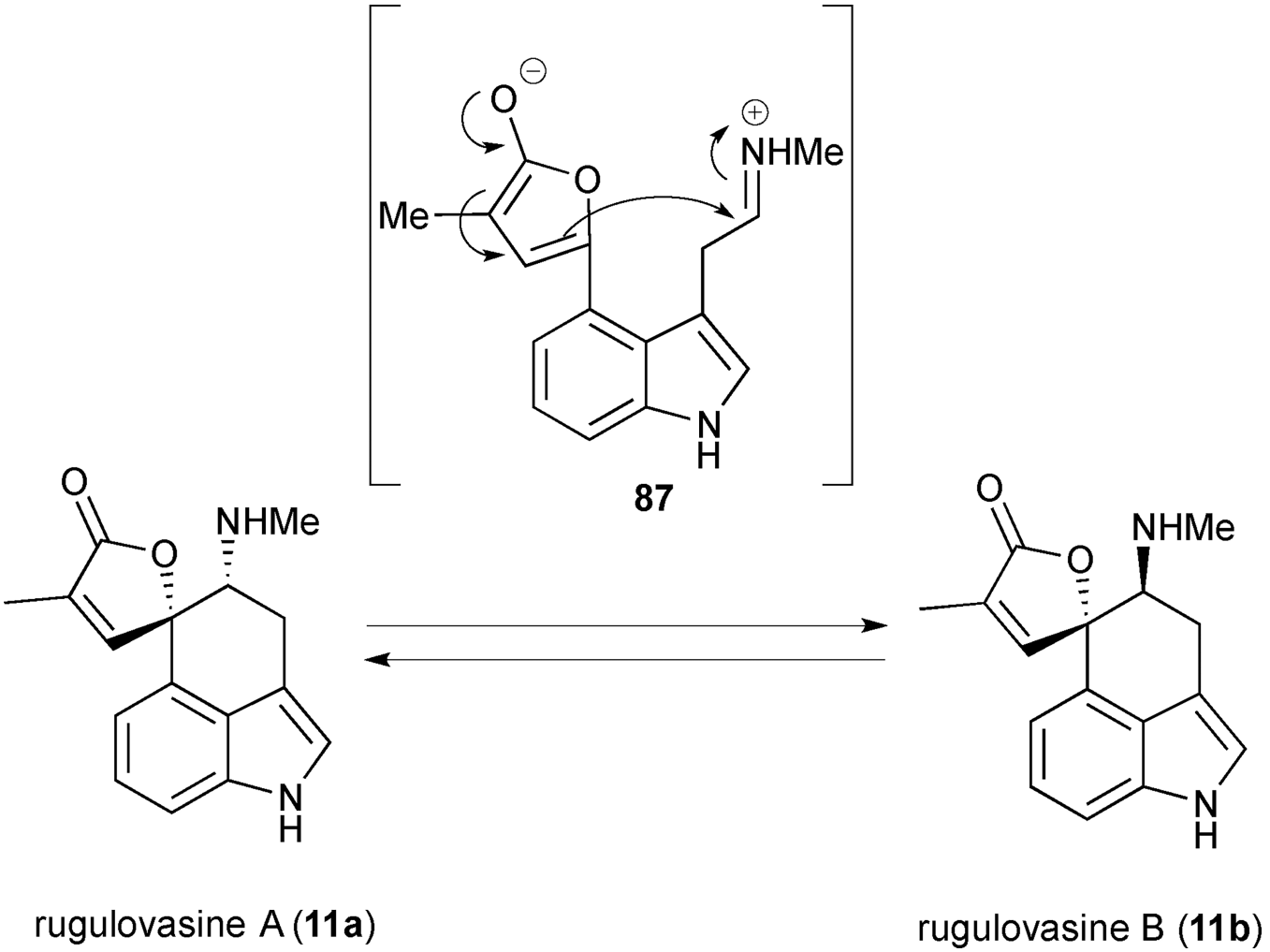

Figure 11.
Mannich mechanism for interconversion of rugulovasines A (**11a**) and B (**11b**)

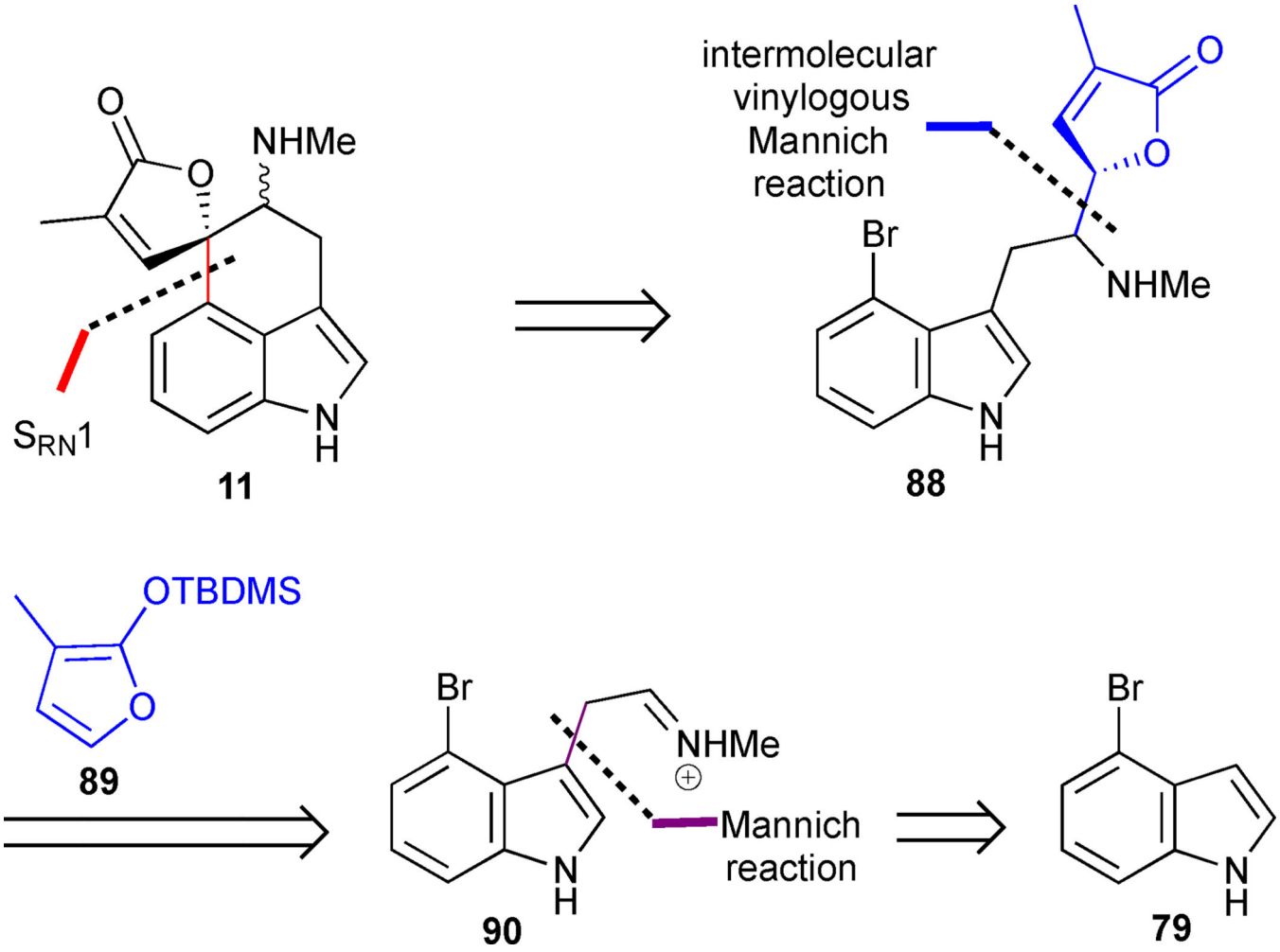

Figure 12.

Retrosynthetic analysis of Martin's approach to rugulovasines A (**11a**) and B (**11b**) based on an intermolecular Mannich strategy

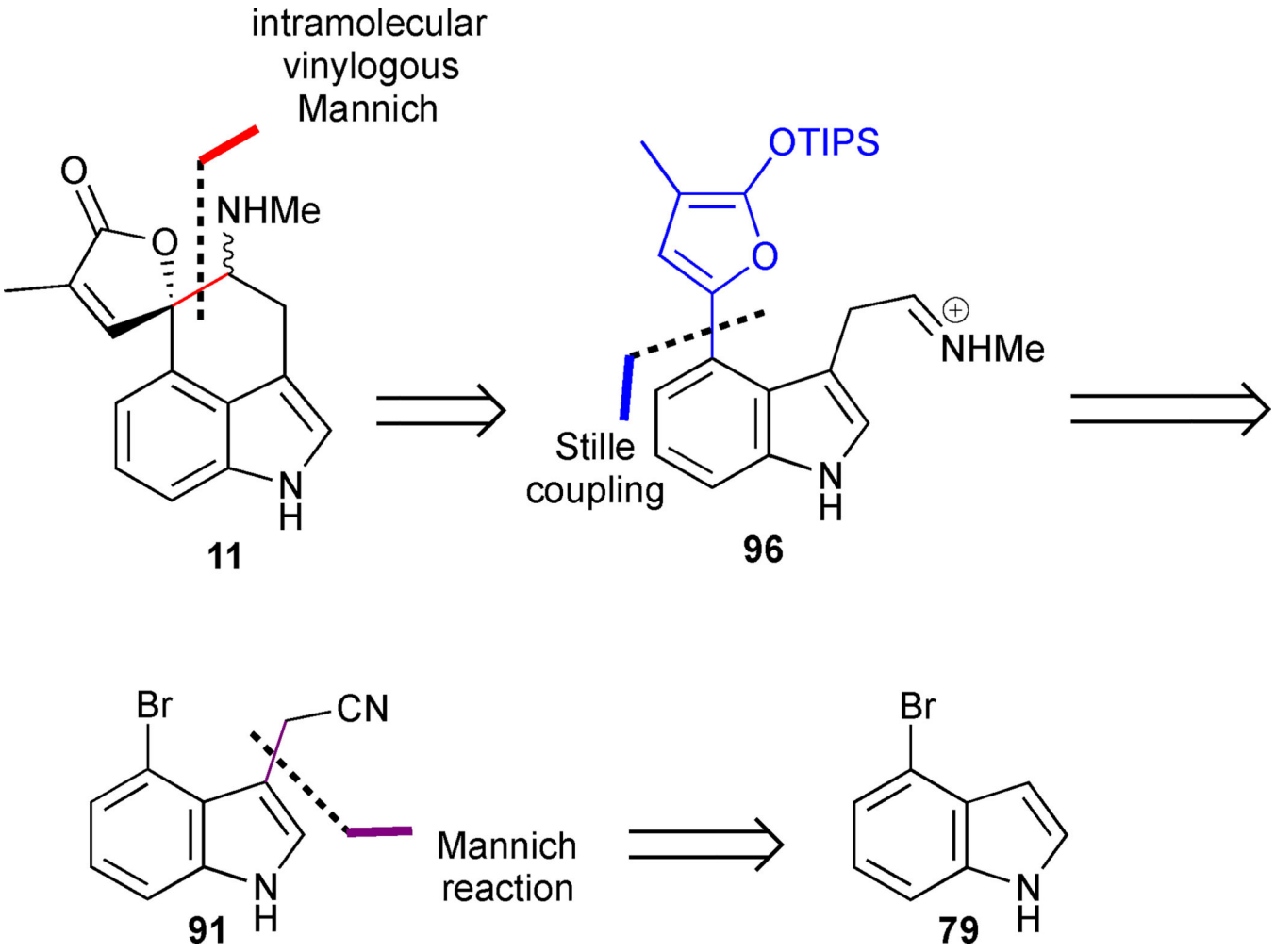

Figure 13.

Second retrosynthetic analysis of Martin's approach to rugulovasines A (**11a**) and B (**11b**) based on an intramolecular Mannich strategy

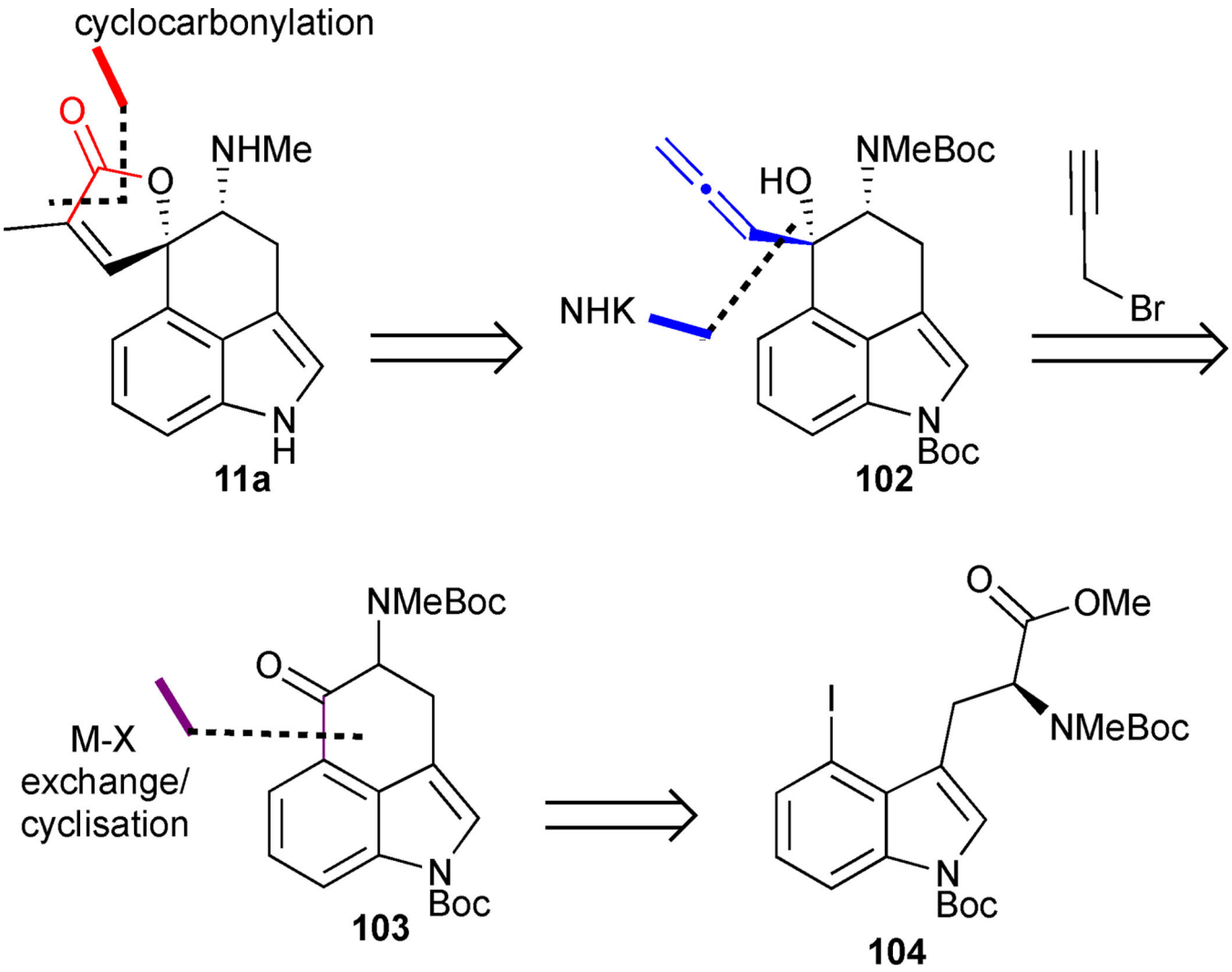

Figure 14.
Retrosynthetic analysis of Jia's approach to rugulovasine A (**11a**)

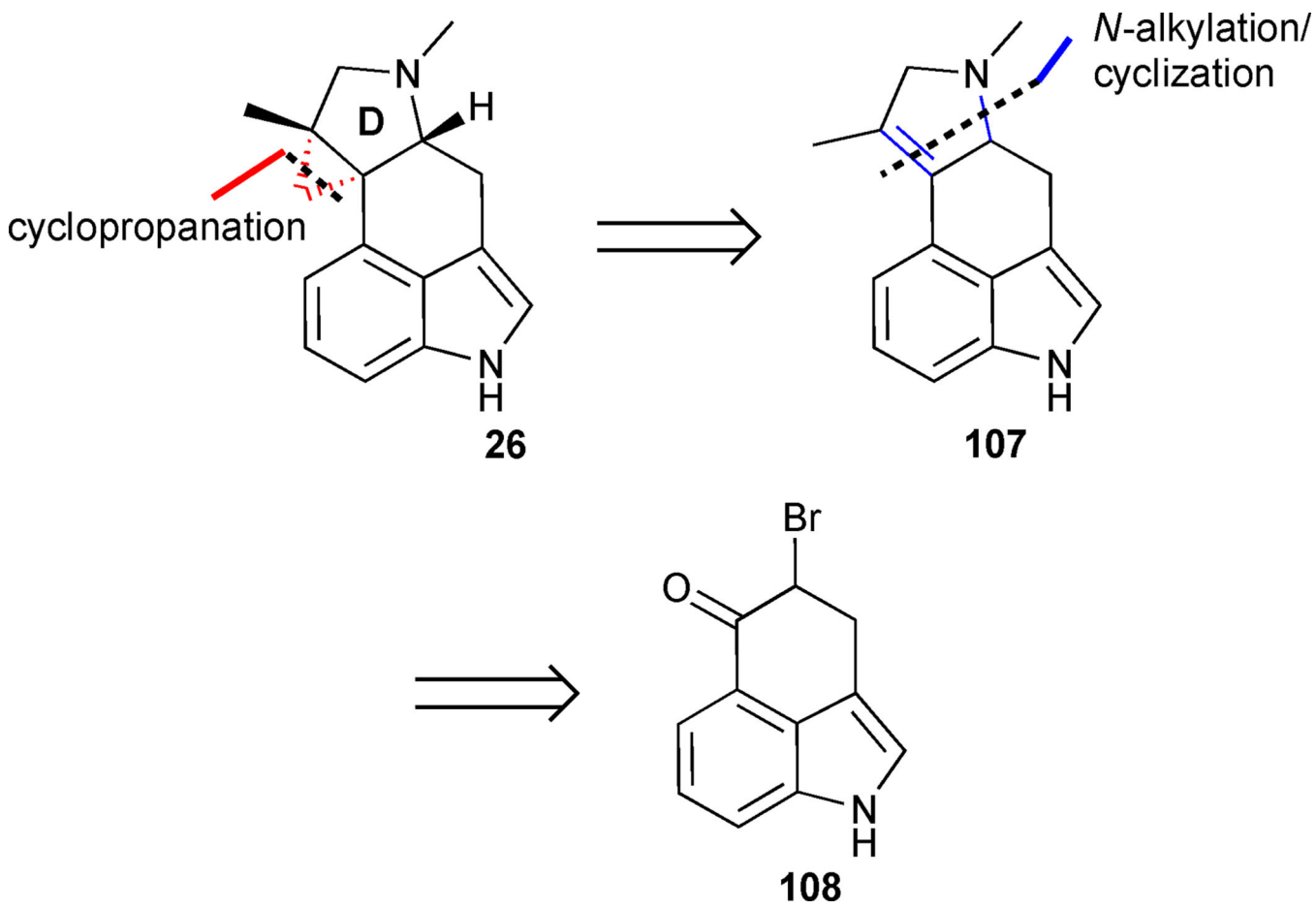

Figure 15.
Retrosynthetic analysis of Szántay's approach to cycloclavine (**26**)

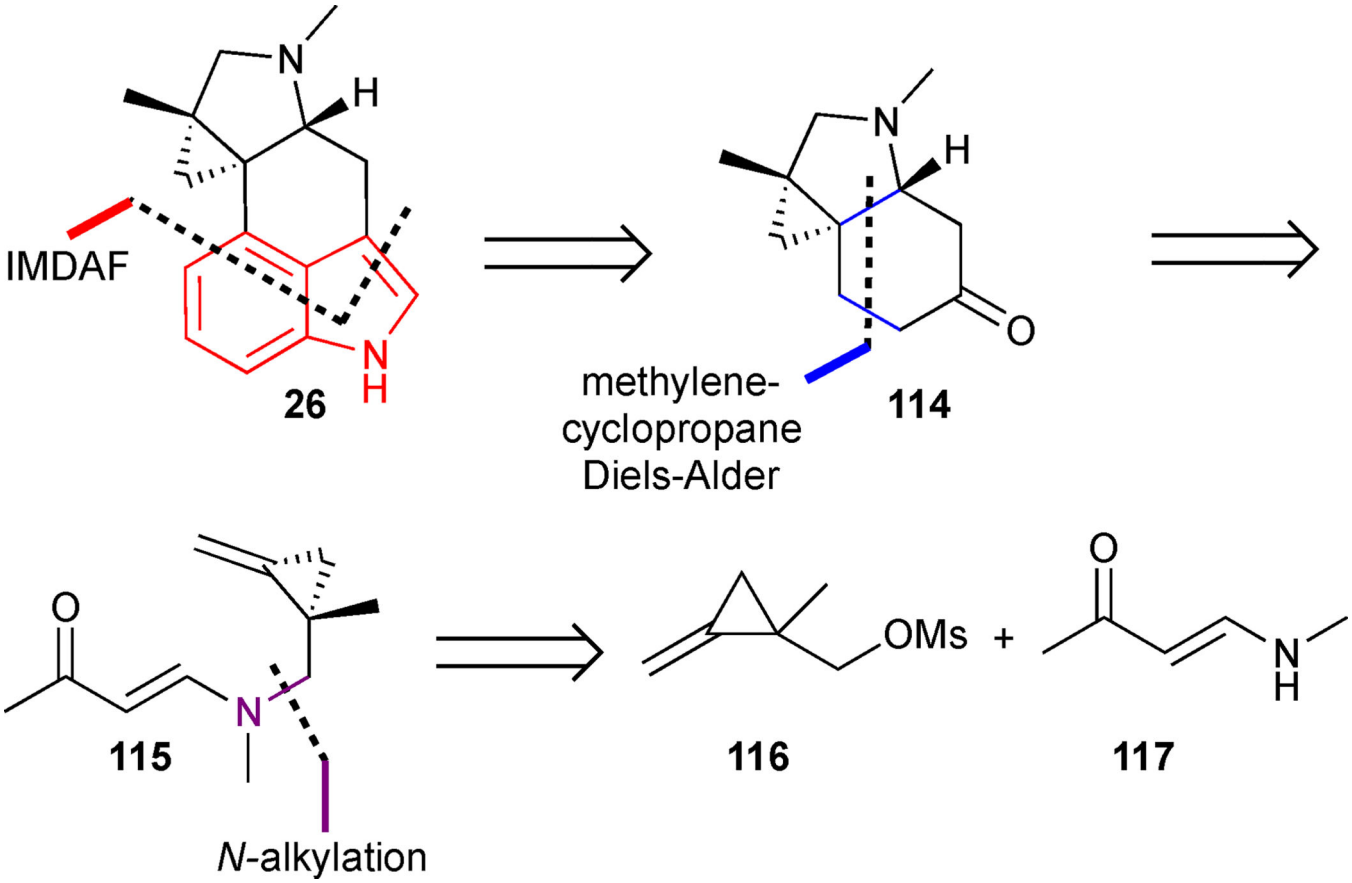

Figure 16.
Retrosynthetic analysis of Wipf's approach to cycloclavine (**26**)

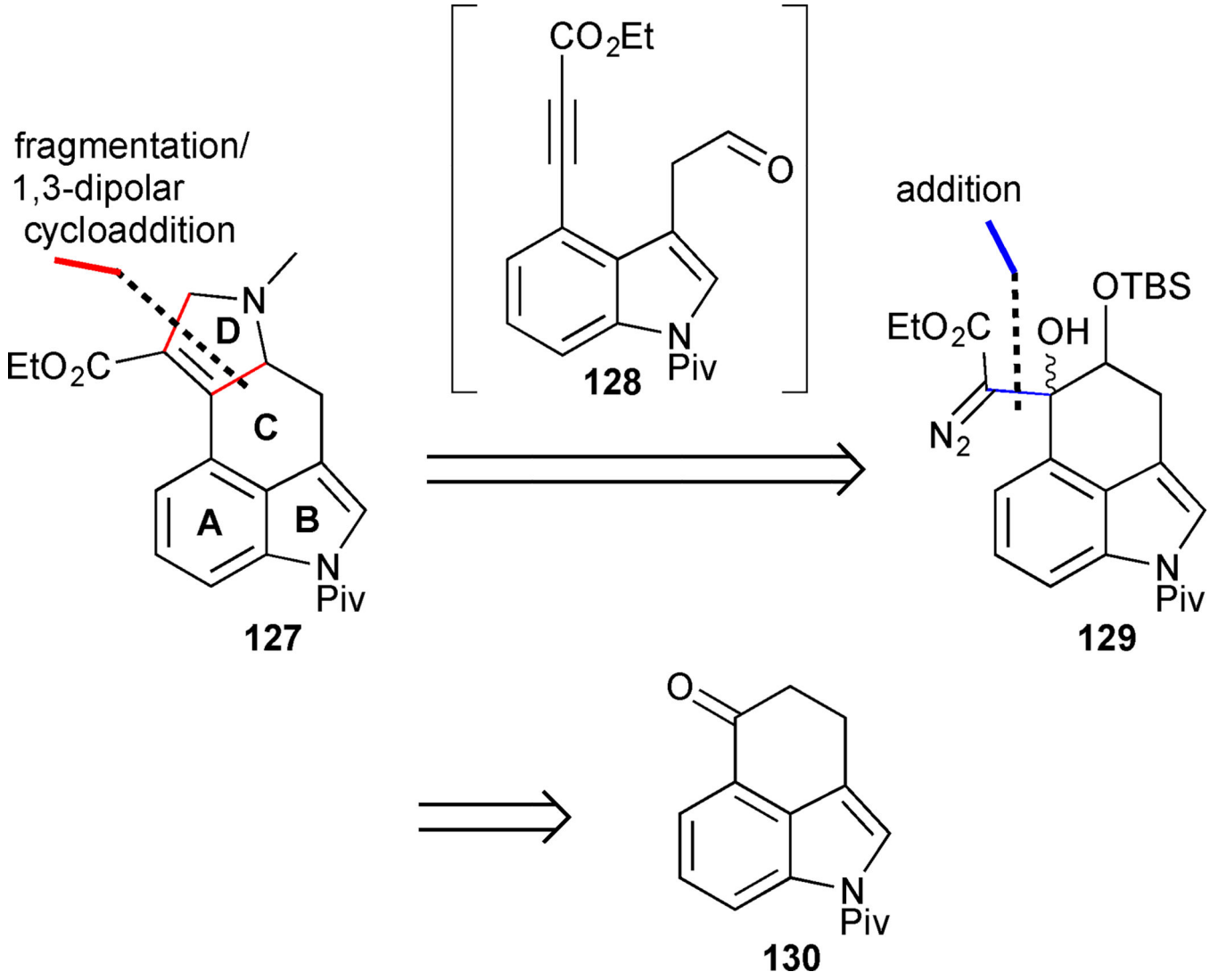

Figure 17.
Retrosynthesis of Brewer's approach to cycloclavine (**26**)

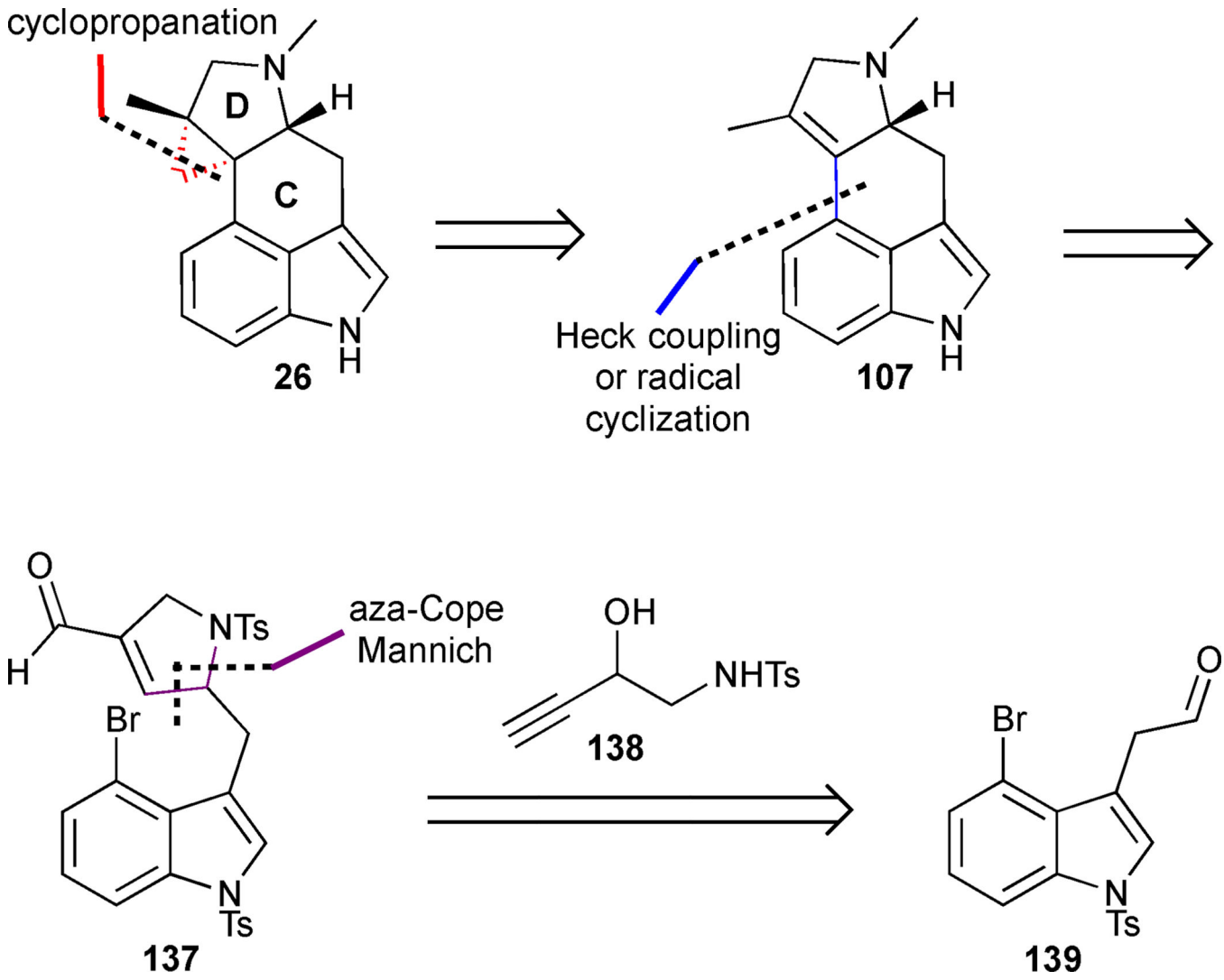

Figure 18.
Retrosynthetic analysis of Cao's formal synthesis of cycloclavine (**26**)

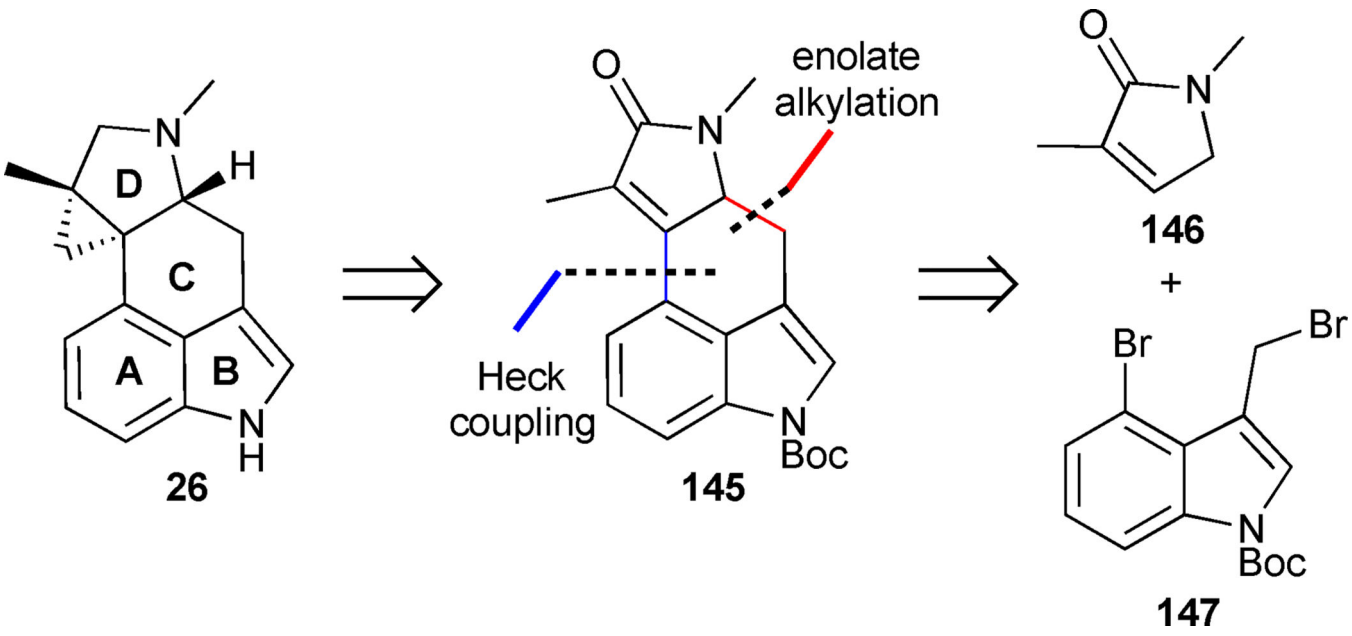

Figure 19.
Retrosynthetic analysis of Opatz's formal synthesis of cycloclavine (**26**)

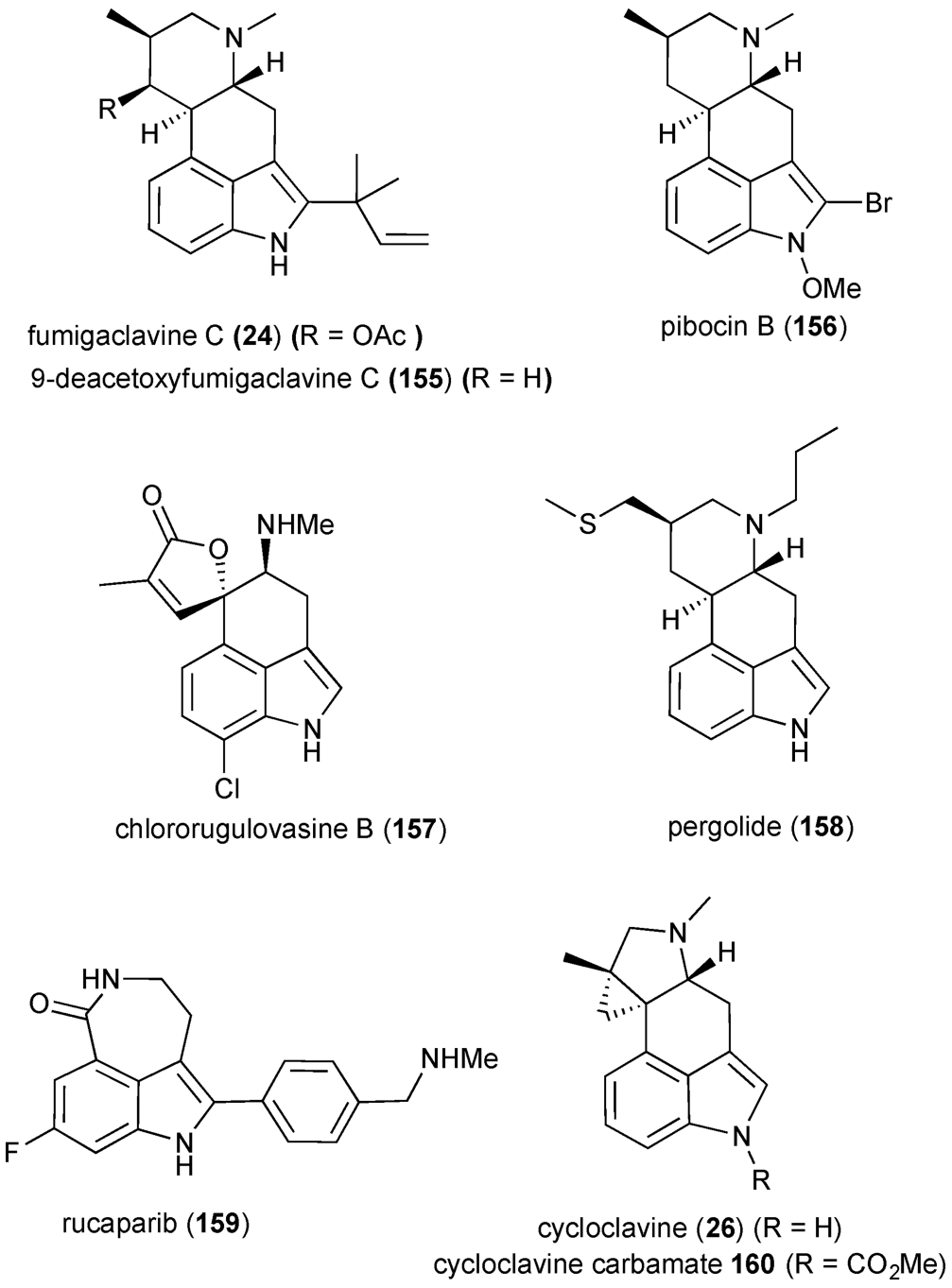

Figure 20.
Biologically active clavine alkaloids

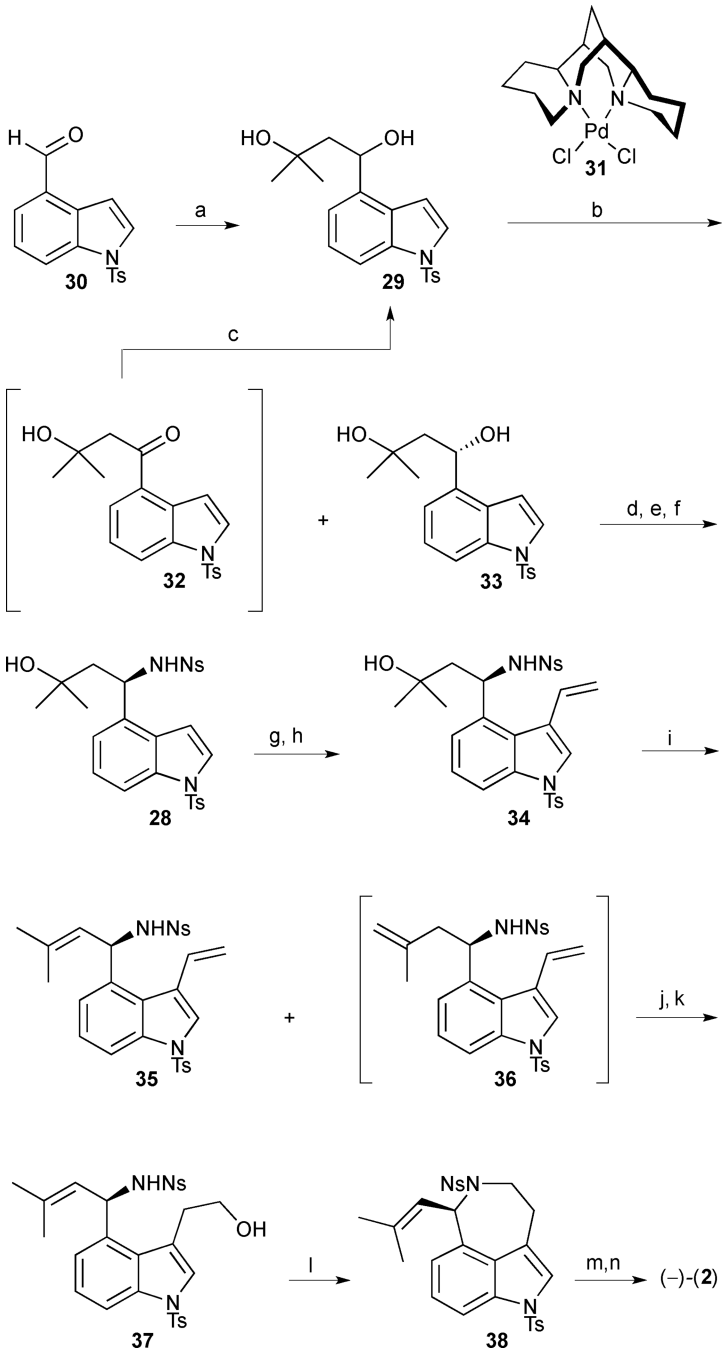

Scheme 1.

(−)-Aurantioclavine (**2**). *Reagents and conditions*: (a) isobutylene oxide, lithium 4,4'-di*tert*-butylbiphenylide (LiDBB), THF, −78 °C, 69%; (b) [Pd((−)-sparteine)Cl_2] (**31**) (10 mol%), O_2 (1 atm), (−)-sparteine (40 mol%), 3Å MS, *t*-BuOH, 40 °C to 70 °C, 98 h, **32,** 51%, and **33**, 37% (96% ee); (c) $LiAlH_4$, THF, −78 °C, 95%; (d) HN_3, PBu_3, DIAD, PhMe, −78 °C to −20 °C, 80%; (e) H_2, cat. Pd/C, HCl, MeOH, 23 °C; (f) *o*-NsCl, Et_3N, CH_2Cl_2, 0 °C to 23 °C, 92% (2 steps); (g) $PyHBr_3$, CH_2Cl_2, 0 °C to 23 °C, 72%; (h) tributylvinyltin, $Pd(PPh_3)_4$ (20 mol%), PhMe, 100 °C, 75%; (i) $POCl_3$, pyridine, 0 °C to 23 °C, 95%, **35**:**36**

(68:32); (j) 9-BBN, THF, 23 °C (k) NaOH, H_2O_2, THF/EtOH/H_2O, 0 °C to 23 °C, 48% (2 steps); (l) DIAD, PPh_3, PhMe, 0 °C, 95%; (m) PhSH, K_2CO_3, DMF, 23 °C, 53%; (n) TBAF, THF, 70 °C, 68%.

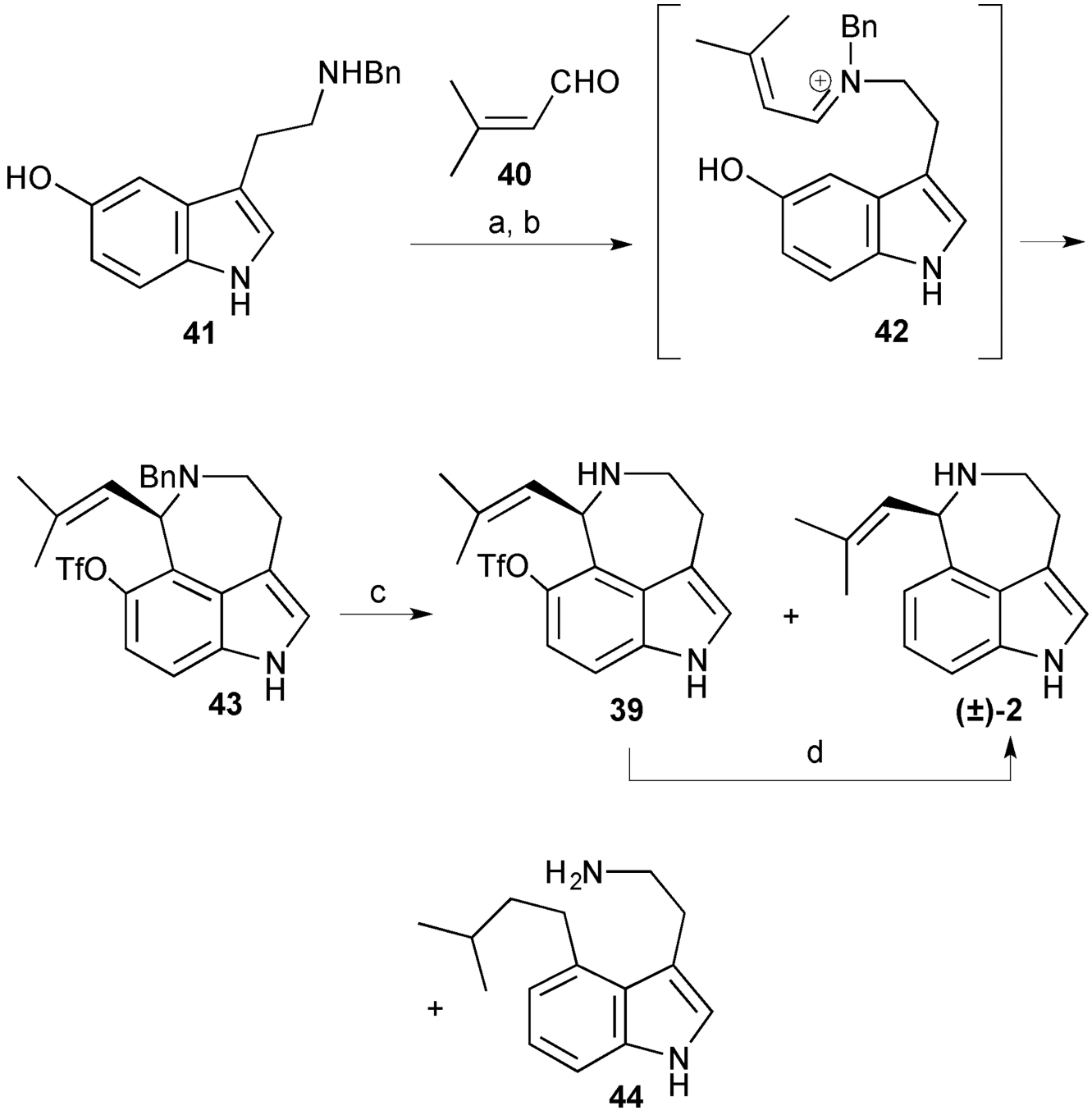

Scheme 2.

(±)-Aurantioclavine. *Reagents and conditions*: (a) NEt_3, MeOH (1:1), room temperature, 10 h; (b) Tf_2O, NEt_3, CH_2Cl_2, 0 °C, 0.5 h, 60% (2 steps); (c) 10% Pd/C, HCO_2NH_4 (4 equiv.), MeOH, room temperature, 0.5 h, 35% **2**, 18% **39**, 28% **44**; (d) $PdCl_2(PPh_3)_2$, dppp, NEt_3, HCO_2H, DMF, 100 °C, 2 h, 43%.

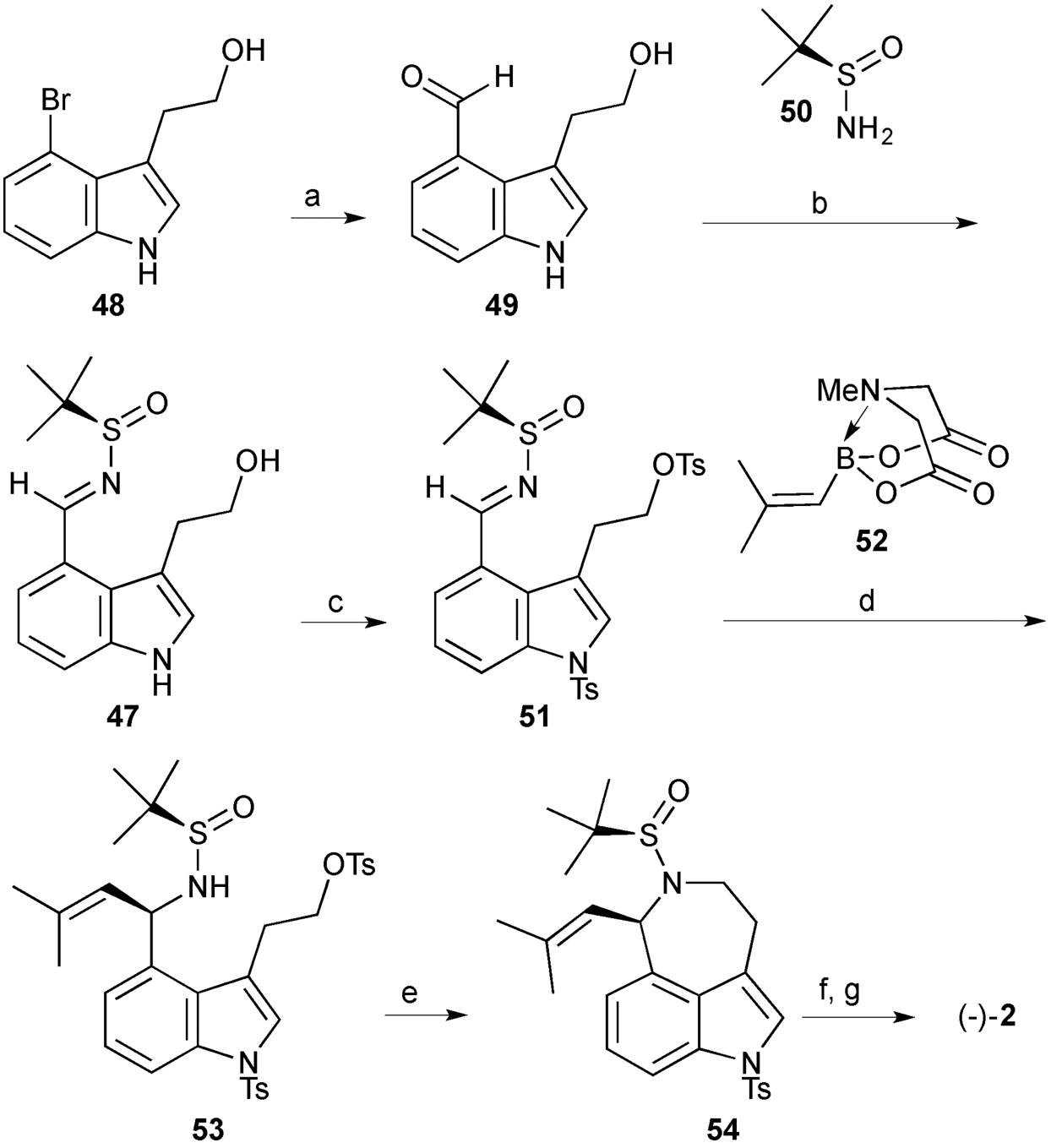

Scheme 3.

(−)-Aurantioclavine (**2**). *Reagents and conditions*: (a) TMSCl, $Pd(OAc)_2$ (0.5 mol%), $Pd(Ad)_2Bu$ (1.5 mol%), H_2/CO (2: 1), TMEDA, 100 °C, PhMe; (b) *N*-t-Butylsulfinamide **50**, $Ti(OEt)_4$, THF, 53% (2 steps); (c) TsCl, NEt_3, DMAP, −20 °C, CH_2Cl_2, 78%; (d) MIDA boronate **52** (2 equiv.), $[Rh(OH)(cod)]_2$ (2.5 mol%), dppbenz (5.0 mol%), K_3PO_4 (2 equiv.), H_2O/ dioxane (3:2), 60 °C, 78%, *dr* 97:3; (e) NaH, THF, 85%; (f) HCl, MeOH; (g) Mg, MeOH, 99% (2 steps)

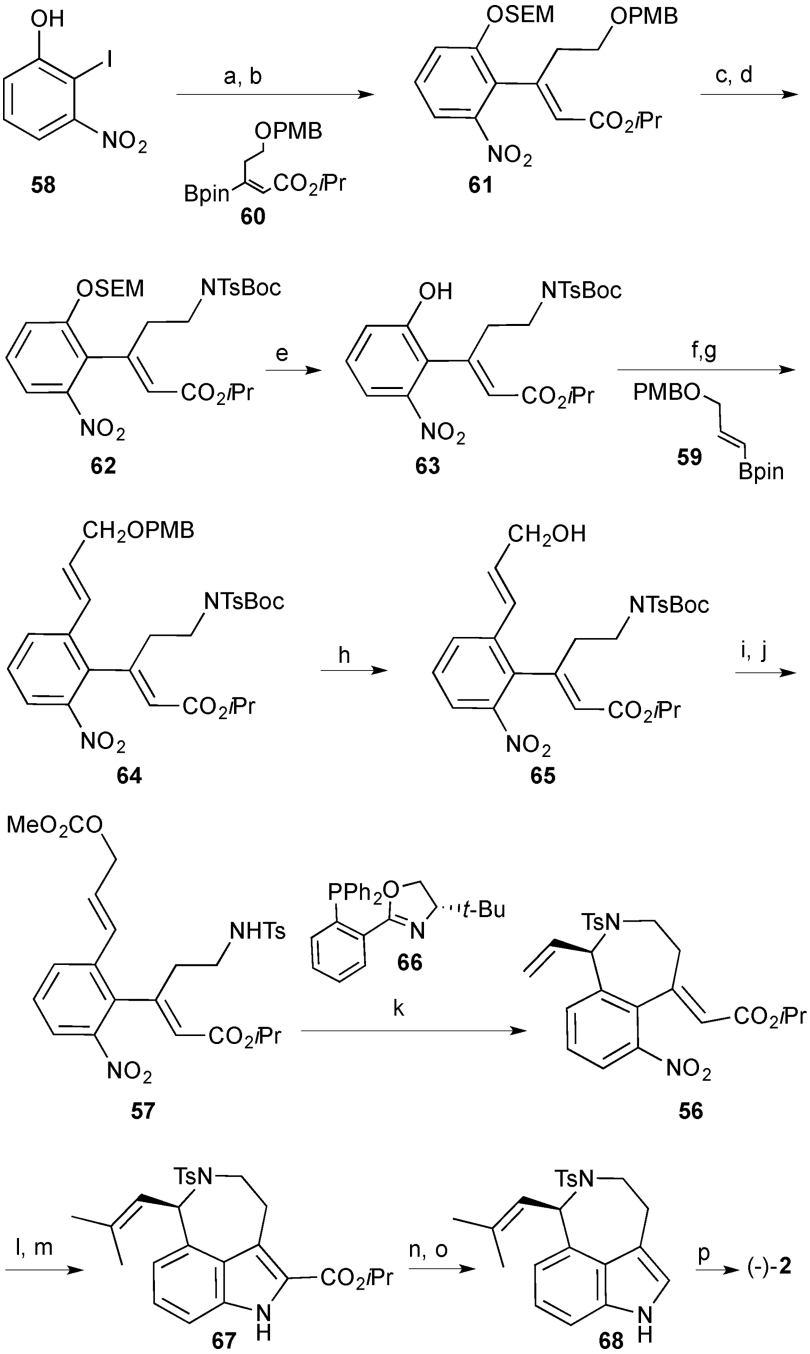

Scheme 4.

(−)-Aurantioclavine (**2**). *Reagents and conditions*: (a) SEMCl, Cs_2CO_3, CH_3CN, 96%; (b) $Pd(OAc)_2$, SPhos, Na_2CO_3, DMF, 100 °C, vinylborane **60**; (c) DDQ, CH_2Cl_2/H_2O, 82% (2 steps); (d) BocNHTs, DIAD, PPh_3, THF, 88%; (e) conc. HCl, MeOH, CH_2Cl_2, 70%; (f) $PhNTf_2$, Et_3N, CH_2Cl_2, 87%; (g) vinylborane **59**, $Pd(PPh_3)_4$, Na_2CO_3, EtOH/PhMe/H_2O, 100 °C; (h) DDQ, CH_2Cl_2/H_2O, 84% (2 steps); (i) $ClCO_2Me$, pyridine, $CHCl_3$, reflux; (j) TFA, $CHCl_3$, reflux, 87% (2 steps); (k) *t*Bu-PHOX **66** (45 mol%), $Pd_2(dba)_3$ (15 mol%), Bu_4NCl (0.30 equiv.), 0 °C, CH_2Cl_2, 72 h, 77% (95% ee); (l) 2-methyl-2-butene, Grubbs 2nd

generation catalyst., 40 °C; (m) $P(OEt)_3$, 170 °C, 78% (2 steps); (n) NaOH (aq), THF/MeOH, reflux; (o) Cu, quinoline, 190 °C, 68% (2 steps); (p) Na/ naphthalene, DME, −78 °C, 90%

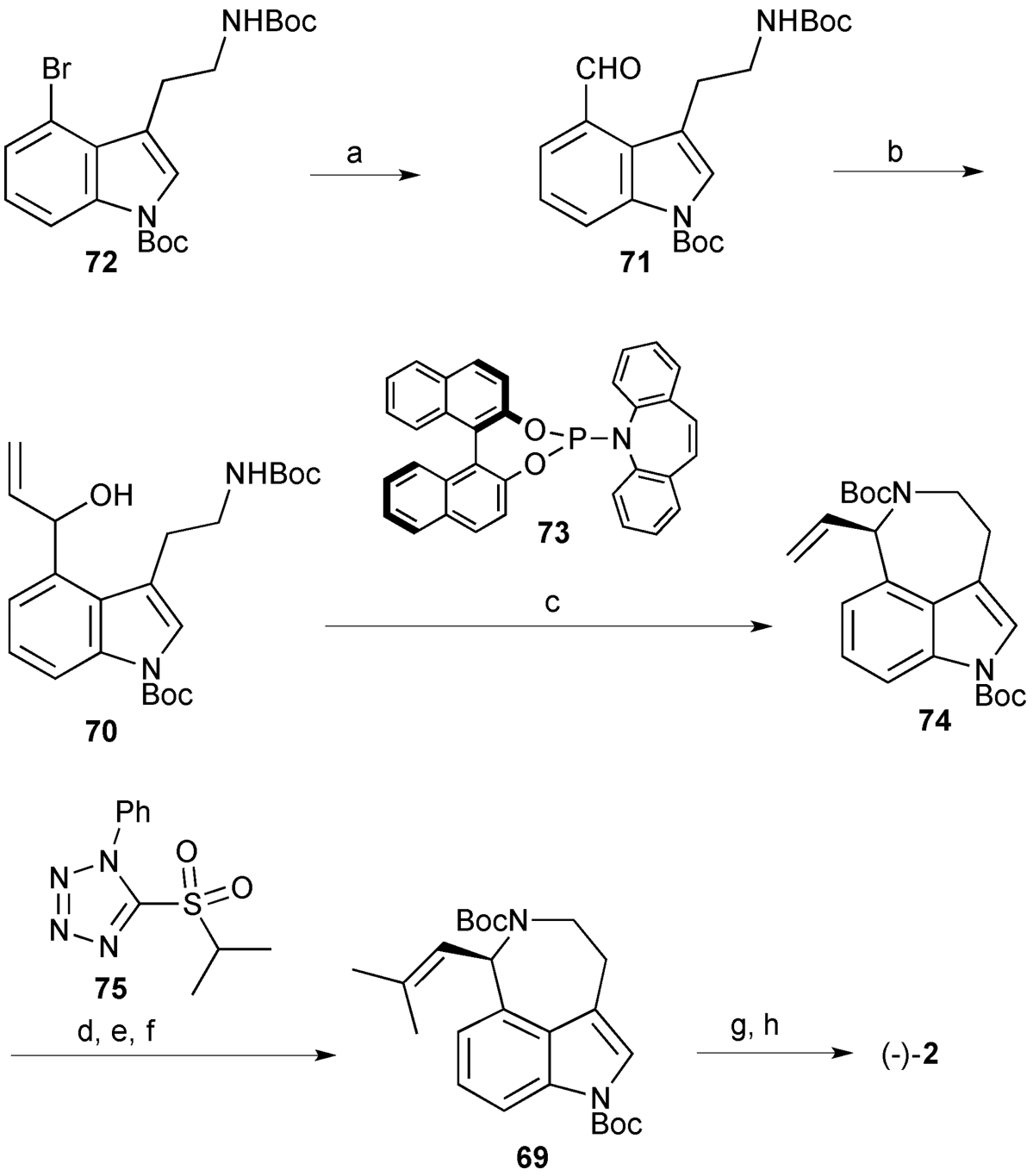

Scheme 5.

(−)-Aurantioclavine (**2**). *Reagents and conditions*: (a) *n*-BuLi, DMF, THF, −78°C, 70%; (b) vinyl magnesium bromide, THF, −78°C, 5 min, 85%; (c) **73** (21 mol%), [{Ir(cod)Cl}$_2$] (4 mol%), Sc(OTf)$_3$ (20 mol%), DCE, 86% yield (93% ee); (d) AD-mix-α, *t*-BuOH/ H_2O, room temperature, 5 d (e) $NaIO_4$, MeOH/ H_2O, 0 °C, 5 min; (f) LiHMDS, tetrazole **75**, THF, −78 °C, 70% BRSM (3 steps); (g) TMSOTf, lutidine, CH_2Cl_2, 90%; (h) K_2CO_3, MeOH/ H_2O, 100 °C, 90%.

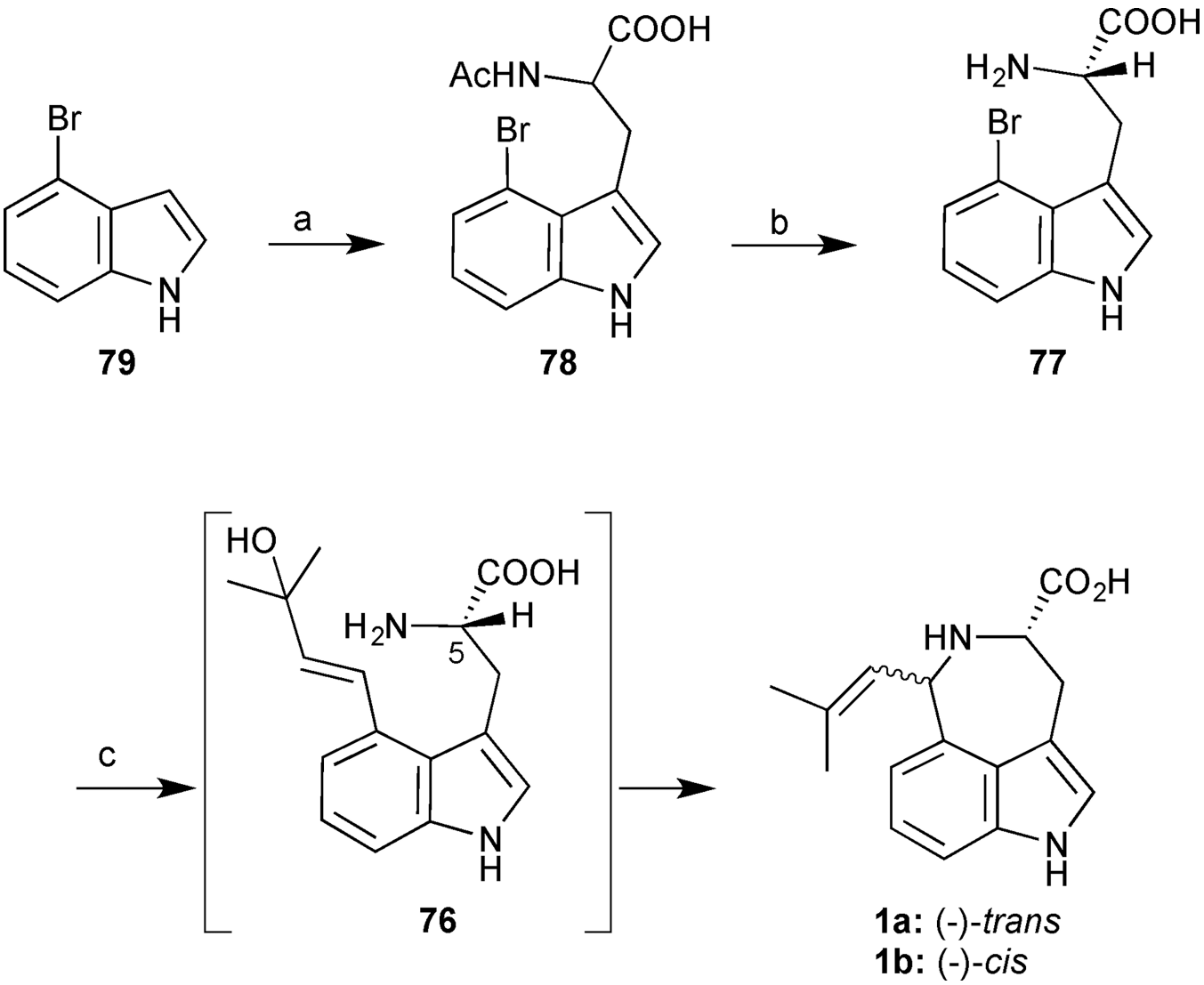

Scheme 6.

(−)-*trans*-(**1a**) and (−)-*cis*-clavicipitic acid (**1b**). *Reagents and conditions*: (a) *DL*-serine, AcOH, Ac_2O, 80 °C, 71%; (b) *Aspergillus acylase*, $CoCl_2$•$6H_2O$, NaH_2PO_4 buffer, 37 °C, 2 days, 49% (>99% *ee*); (c) 2-methyl-3-buten-2-ol, $Pd(OAc)_2$ (0.1 equiv.), TPPTS (0.2 equiv.), K_2CO_3, H_2O, 130 °C, 8 h then 60% AcOH (aq), 60 °C, 2 h, 61%.

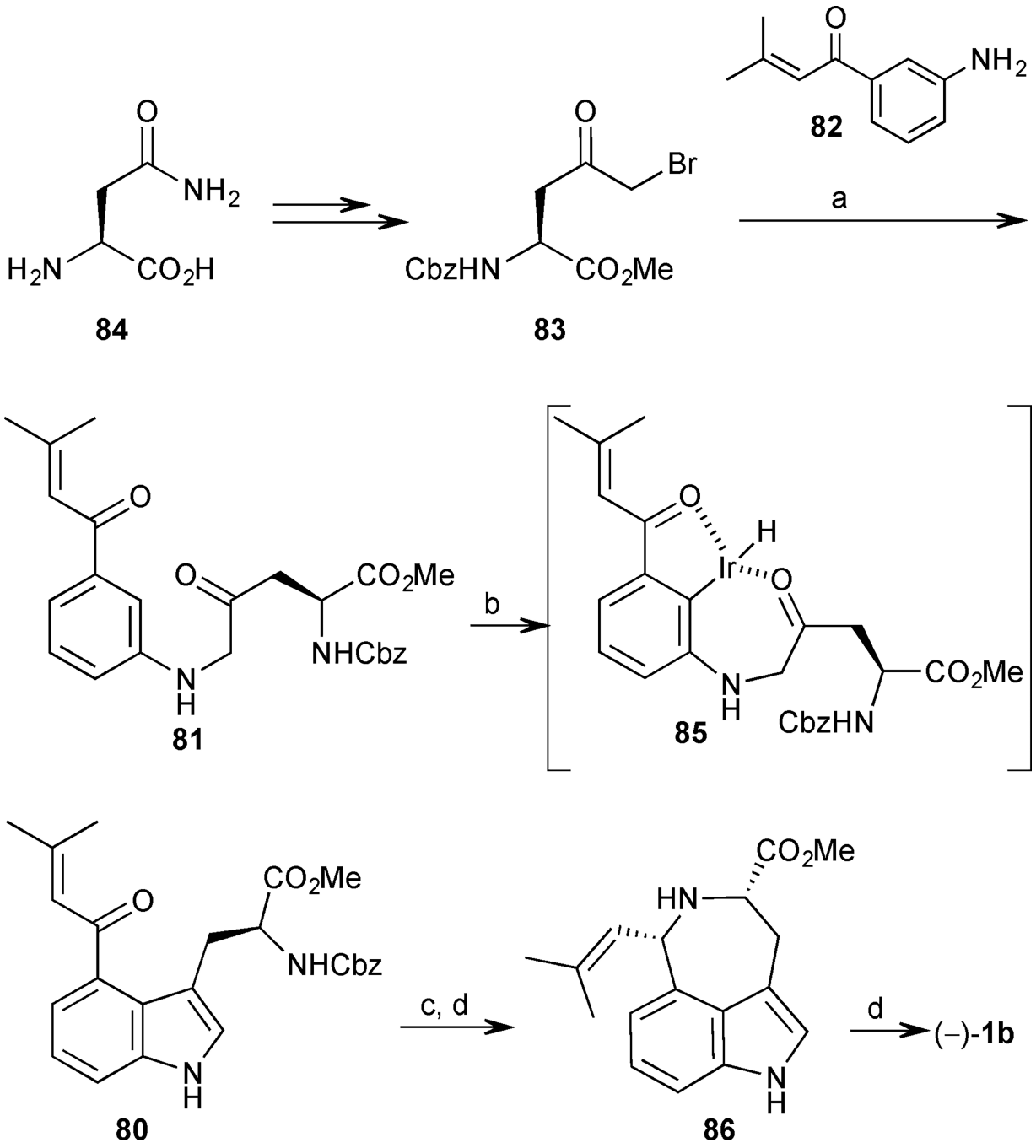

Scheme 7.

(−)-*cis* Clavicipitic acid. *Reagents and conditions*: (a) **82** (3 equiv.), K_2CO_3 (2 equiv.), DMF, room temperature, 3.5 h, 83%; (b) $[Ir(cod)_2]$BARF (10 mol%), *rac*-BINAP (10 mol%), PhCl, 135 °C, 15 h, 79%; (c) HBr/ AcOH (10 equiv.), room temperature, overnight; (d) $NaBH(OAc)_3$, (4.2 equiv.), Et_3N, CH_2Cl_2, room temperature, 24 h, 53% (2 steps); (d) KOH, $MeOH/H_2O$ (2:1), room temperature, 15 min (ref [46])

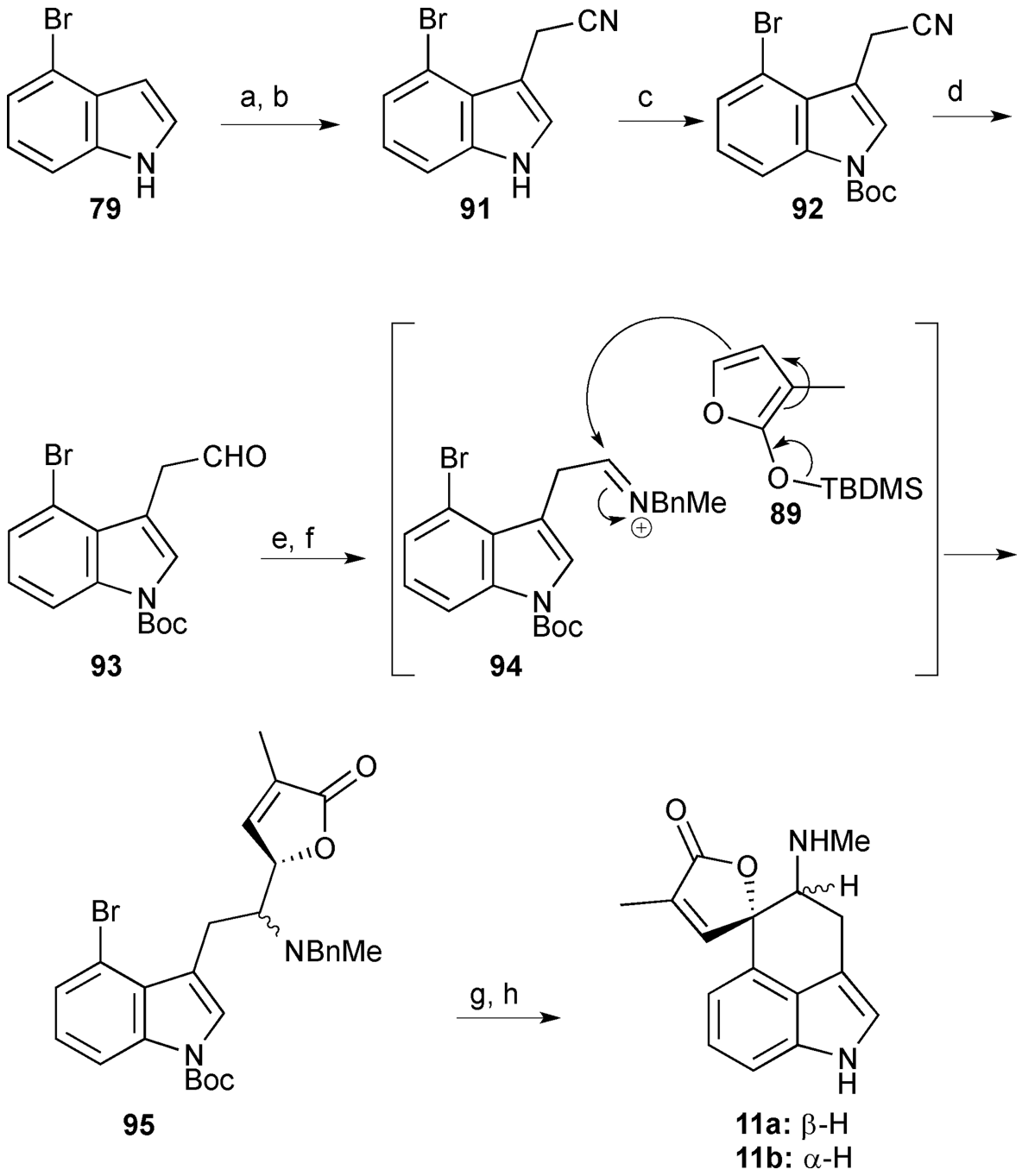

Scheme 8.

Rugulovasine A (**11a**) and B (**11b**). *Reagents and conditions*: (a) $HNMe_2$, CH_2O; (b) KCN, aq. DMF (1: 1), 71% (2 steps); (c) $(Boc)_2O$, DMAP, Et_3N, 94%; (d) DIBAL-H, CH_2Cl_2, −78 °C, 45 min then room temperature, 5 h; (e) benzylmethylamine, CH_2Cl_2, room temperature, 8 h; (f) silyloxyfuran **89**, benzene, CSA, reflux, 1 h, 45% (3 steps); (g) KO*t*Bu, NH_3 (liq.), *hν*, 51%; (h) HCl, H_2 (1 atm), 20% $Pd(OH)_2$, EtOH, room temperature, **11a**:**11b** (1:2), 74%.

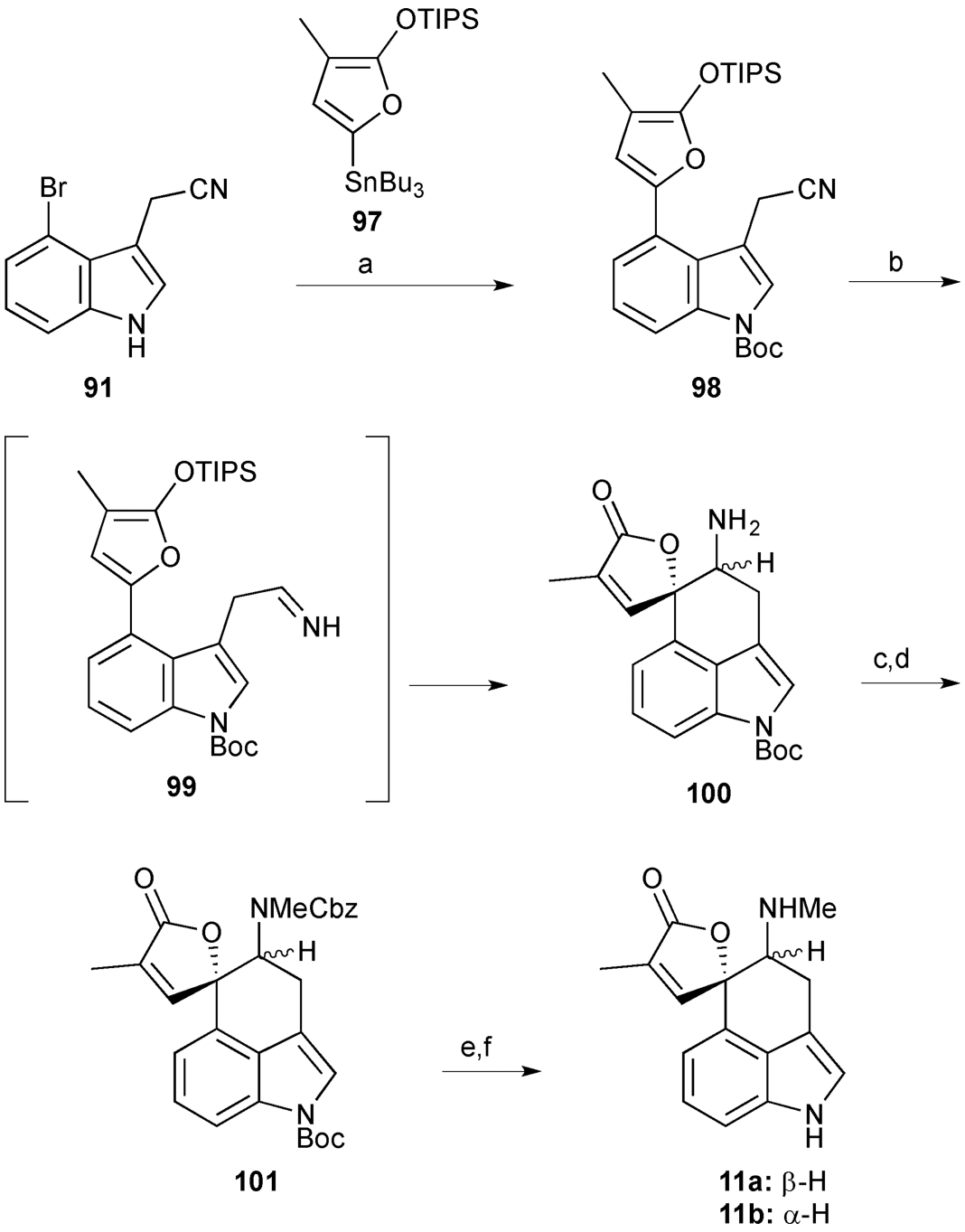

Scheme 9.

Rugulovasines A (**11a**) and B (**11b**). *Reagents and conditions*: (a) furanyl stannane **97**, $Pd(PPh_3)_4$, PhMe, K_2CO_3, reflux, 1 h then $(Boc)_2O$, DMAP, Et_3N, 94%; (b) DIBAL-H, −78 °C to room temperature, then SiO_2, 71%; (c) CBz-OSuc, Et_3N, DMF, room temperature, 26 h; (d) NaH, MeI, DMF, 85% (2 steps); (e) Cs_2CO_3, MeOH; (f) H_2, Pd/C, MeOH-THF, **11a:11b** (2:1), 74% (2 steps).

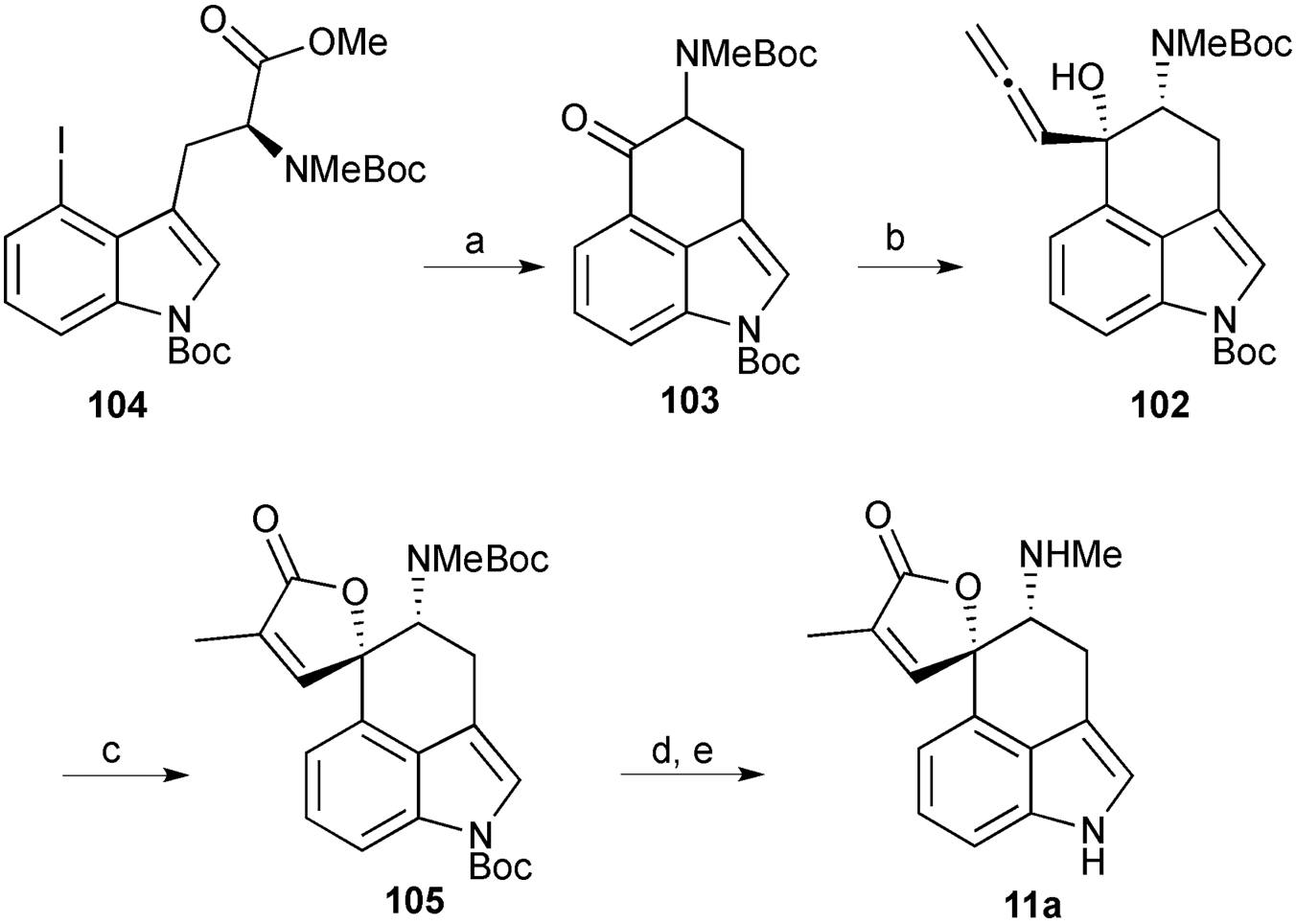

Scheme 10.

Rugulovasine A (**11a**). Reagents and conditions: (a) *t*-BuLi, THF, −78 °C, 80%; (b) propargylbromide, $CrCl_3$, $LiAlH_4$, THF/HMPA, room temperature, 66% (brsm); (c) $Ru_3(CO)_{12}$, 2,4,6-collidine, CO (1 atm), 100 °C, 58%; (d) Cs_2CO_3, MeOH/THF, 75%; (e) TMSOTf, 2,6-lutidine, CH_2Cl_2, 0 °C, 87%

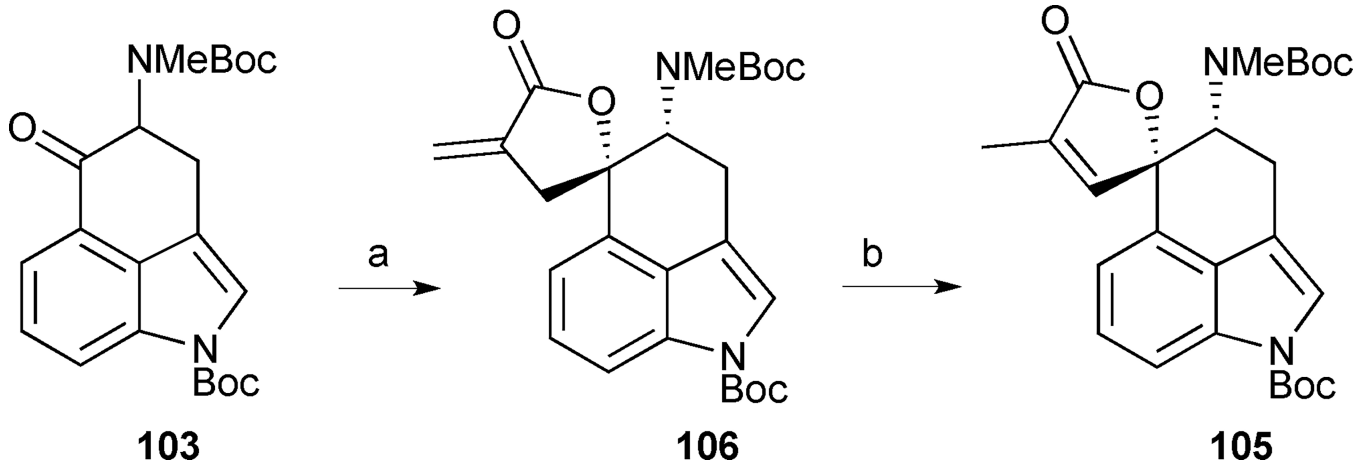

103 **106** **105**

Scheme 11.

Alternative route to intermediate **105**. *Reagents and conditions*: (a) methyl 2-(bromomethyl)acrylate, Zn, I_2, THF, 50 °C, 90%; (b) $Ru_3(CO)_{12}$, Et_3N, dioxane, 100 °C, 2 h, 95%

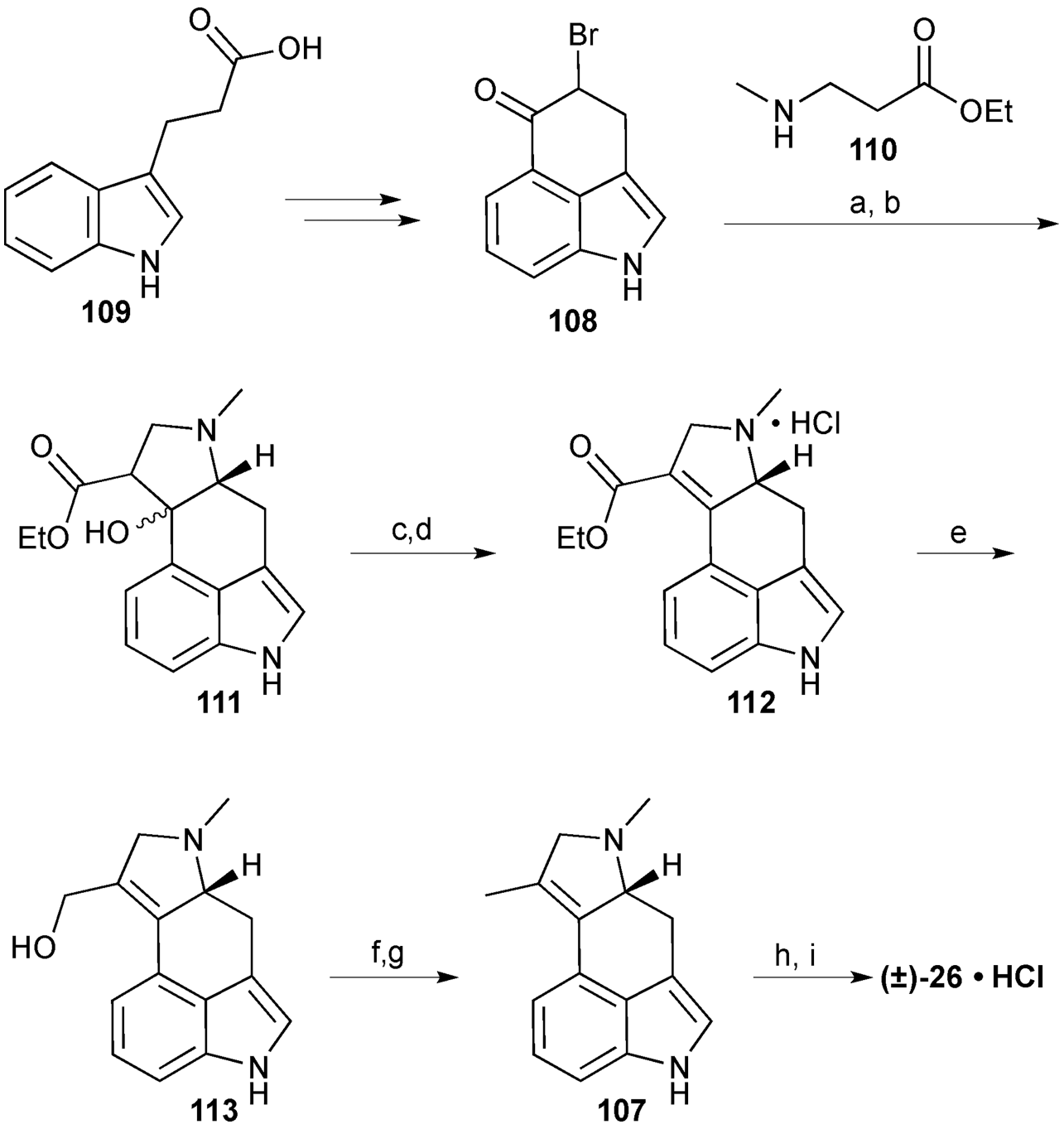

Scheme 12.

Cycloclavine (**26**). *Reagents and conditions*: (a) ethyl 3-(methylamino)propanoate (**110**), THF, 48%; (b) LiHMDS, THF, −70 °C, 50%; (c) $POCl_3$, pyridine, 120 °C; (d) HCl, EtOH, 25%; (e) $LiAlH_4$, Et_2O, 90 %; (f) SO_3•Py, THF; (g) $LiAlH_4$, Et_2O, 62% (2 steps); (h) CH_2N_2, $Pd(OAc)_2$ (i) HCl in dioxane, CH_2Cl_2/ Et_2O, 32% (brsm).

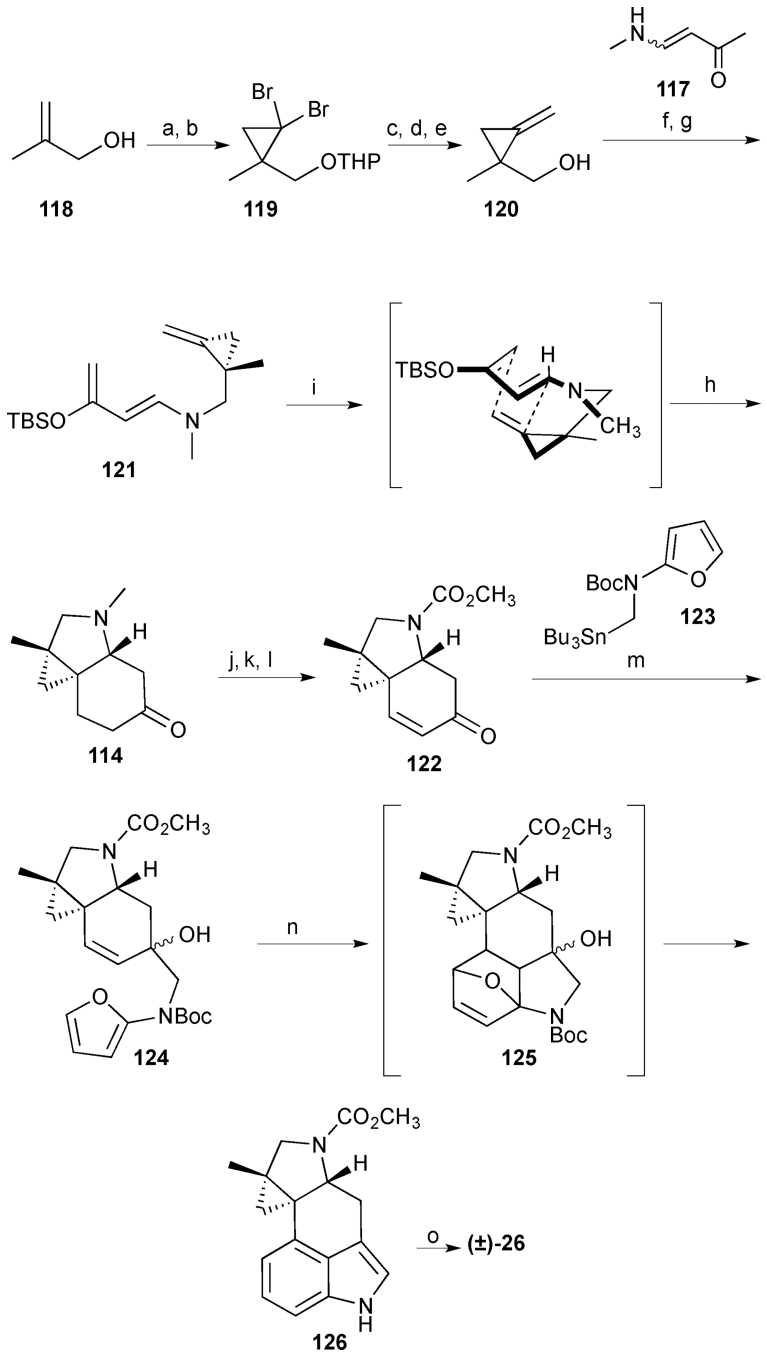

Scheme 13.

Cycloclavine (**26**). *Reagents and conditions*: (a) DHP, HCl (cat.), 90%; (b) $CHBr_3$, Et_3N, cetrimide, NaOH (aq), CH_2Cl_2, 95%; (c) *n*-BuLi, THF, −95 °C then MeI, −95 °C to room temperature, 82%; (d) KO*t*-Bu, DMSO, room temperature, 69%; (e) *p*-TsOH, MeOH, room temperature, 79%; (f) MsCl, Et_3N, CH_2Cl_2, 0 °C, 1 h; (g) amide **117**, NaH, DMF, room temperature, 12 h, 67% (2 steps); (h) NaHMDS, THF, −78 °C then TBSCl; (i) 195 °C, $PhCF_3$, μw, 1 h 52%, (72% brsm) (2 steps); (j) TBAF, THF, room temperature, 85%; (k) MeOC(O)Cl, 70 °C, 3 h, 71%; (l) LDA, THF, −78 °C, 1 h then TMSCl (1.3 equiv.), CH_3CN,

12 h, 67%; (m) **123**, *n*-BuLi, THF, −78 °C, 51%; (n) 180 °C, $PhCF_3$, μW, 30 min, 44% (56% brsm); (o) $LiAlH_4$, THF, 66 °C, 30 min, quantitative.

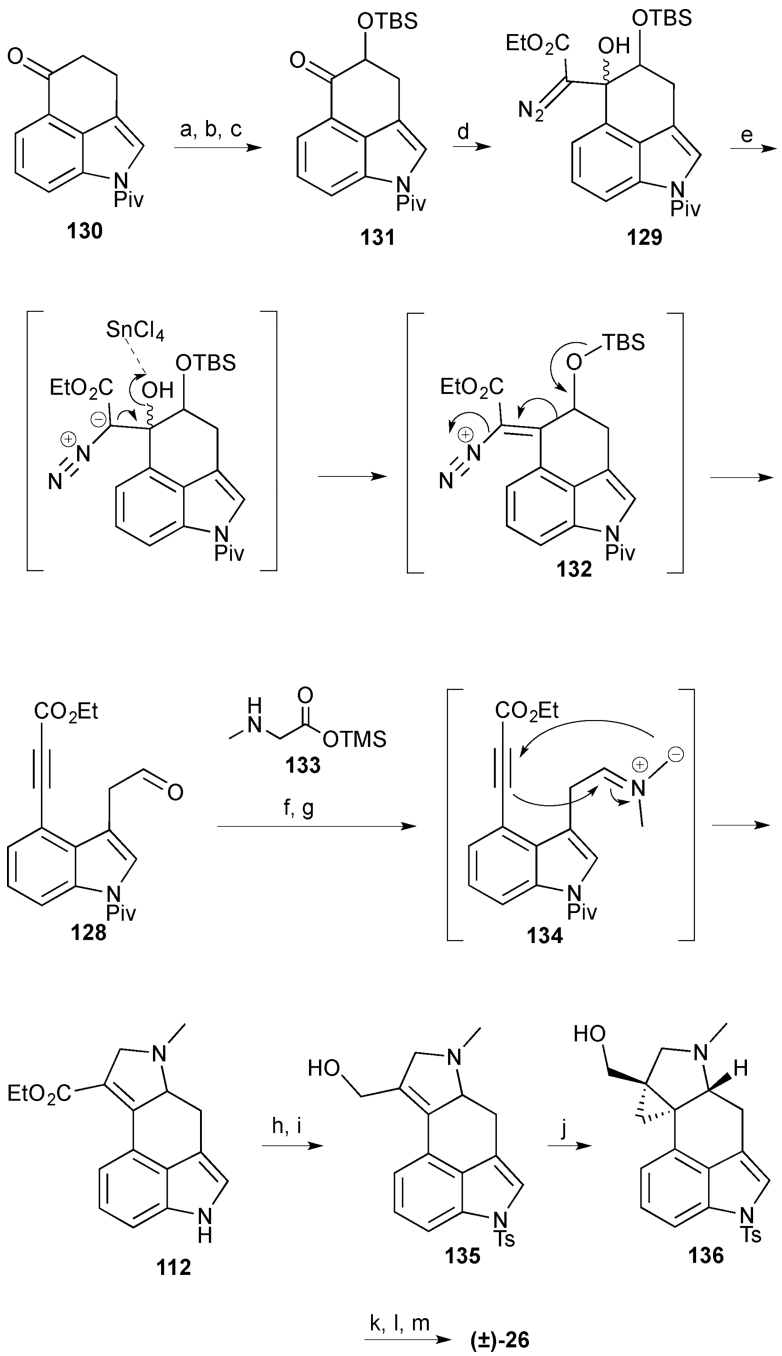

Scheme 14.

Cycloclavine (**26**). *Reagents and conditions*: (a) TBSOTf, Et_3N, CH_2Cl_2, 0 °C to room temperature, 45 min; (b) *m*CPBA, K_2CO_3, CH_2Cl_2, 0 °C, 2 h; (c) TBSCl, DMAP, imidazole, CH_2Cl_2, 6 h, 70% (3 steps); (d) ethyl diazoacetate, LDA, THF, −78 °C, 2 h, 79%; (e) $SnCl_4$, CH_2Cl_2, 0 °C, 10 min, 80%; (f) trimethylsilyl methylglycinate (**133**), PhMe, 0 °C, 30 min then 120 °C, 30 min, 65%; (g) DBU, H_2O, THF, reflux, 19 h; (h) TsCl, Bu_4NHSO_4, KOH, PhMe, 78% (2 steps); (i) DIBAL-H, PhMe, 0 °C to room temperature, 30 min; (j) Et_2Zn, I_2,

CH_3I, CH_2Cl_2, 0 °C to room temperature, 24% (2 steps); (k) MsCl, NEt_3, 0 °C, 1 h; (l) $LiBHEt_3$, THF, 0 °C, 45 min; (m) NaOH, MeOH, reflux, 21% (3 steps)

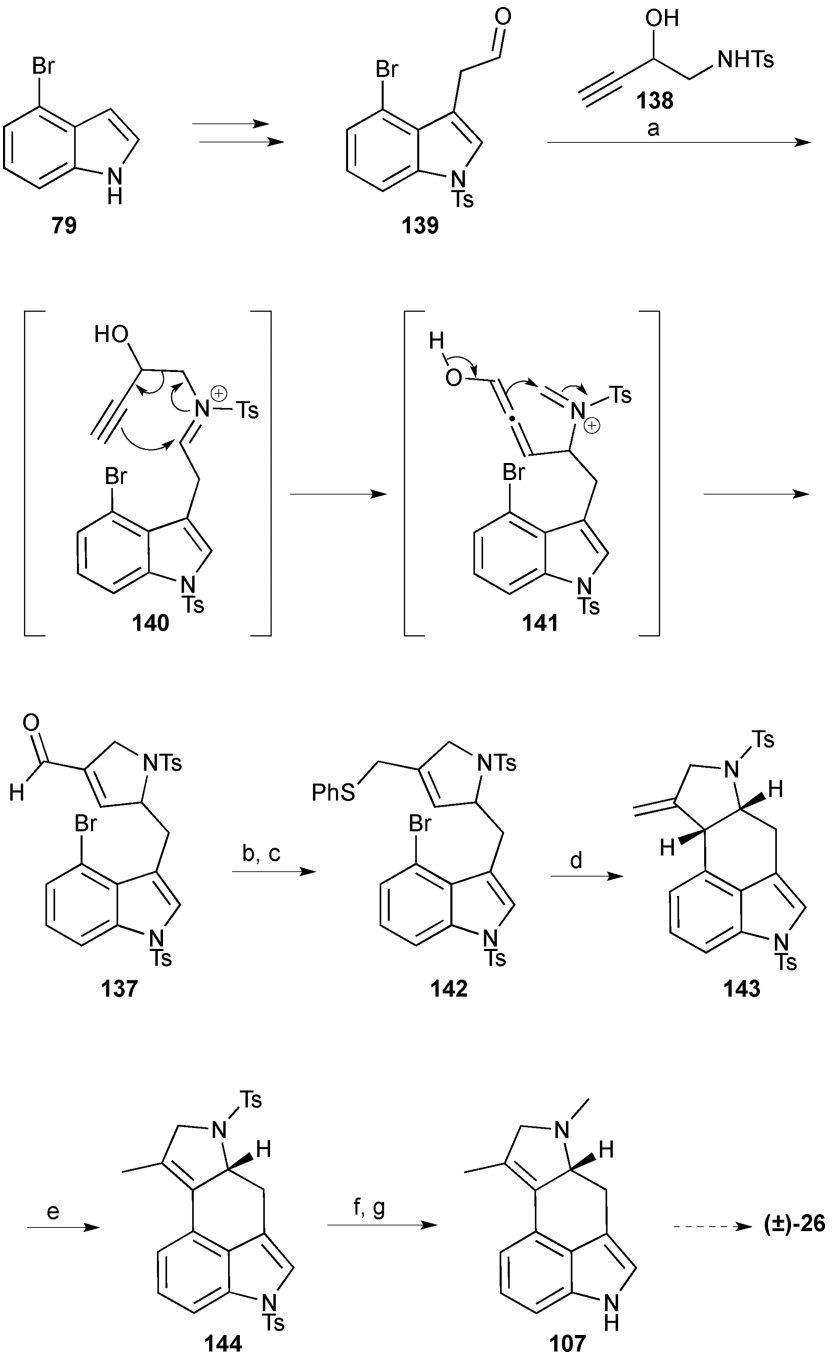

Scheme 15.

Cycloclavine (**26**). *Reagents and conditions*: (a) 2-hydroxy homopropargyl tosylamine (**138**), $FeCl_3$, CH_2Cl_2, reflux, 0.2 h, 83%; (b) $NaBH_4$, $CeCl_3 \cdot 7H_2O$, MeOH, 0 °C; (c) PhSSPh, *n*-Bu_3P, benzene, 81% (2 steps); (d) *n*-Bu_3SnH, AIBN, benzene, reflux, 91%; (e) *p*-$TsOH \cdot H_2O$, benzene, reflux, 63%; (f) sodium naphthalenide, THF, −78 °C; (g) formalin, AcOH, $NaBH_3CN$, THF, 71% (2 steps).

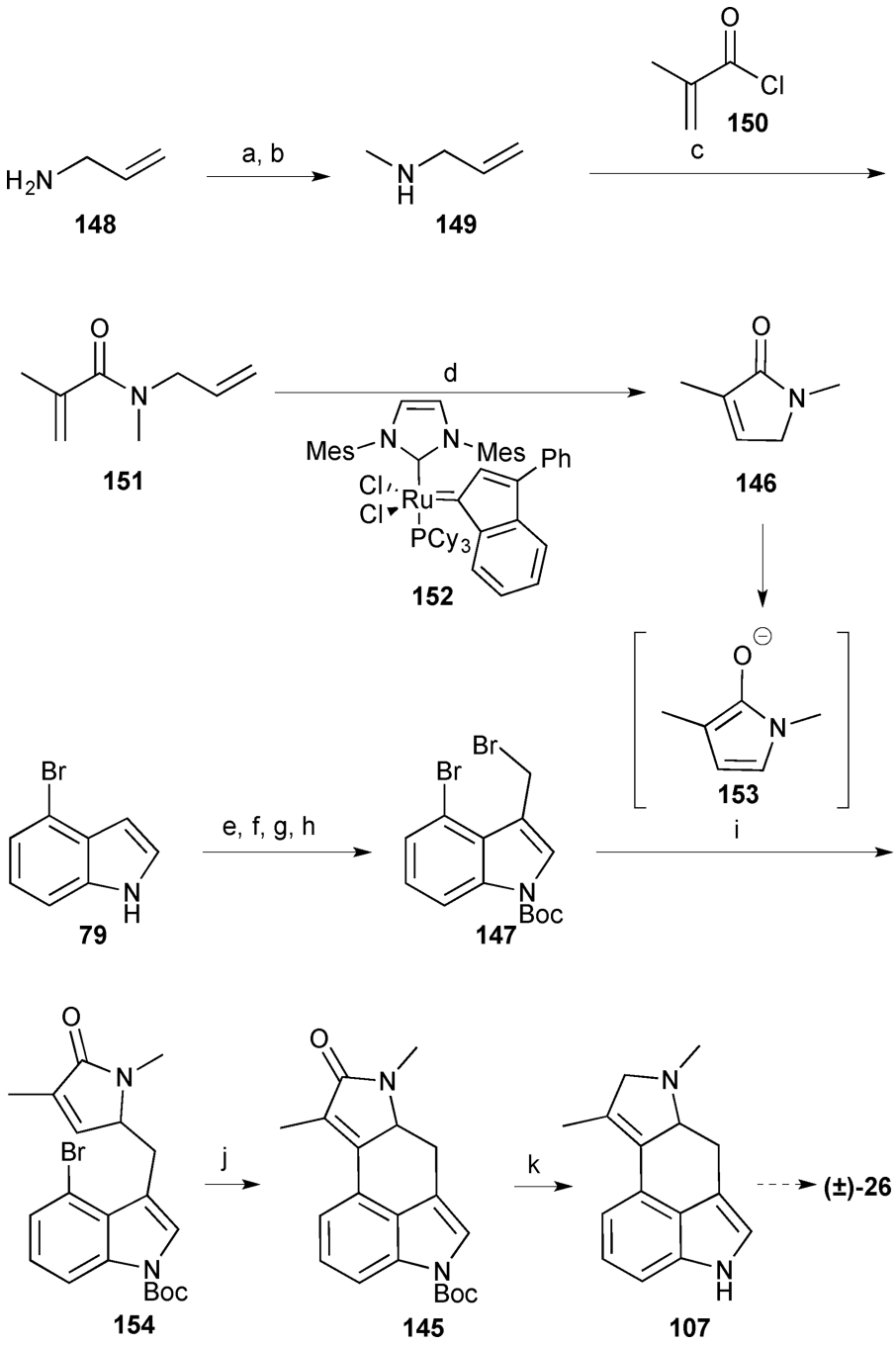

Scheme 16.

Cycloclavine (**26**). *Reagents and conditions*: (a) EtOCHO, 93%; (b) $LiAlH_4$, Et_2O; (c) methacryloyl chloride **150**, NaOH (aq), 79% (2 steps); (d) **152** (1 mol%), PhMe, reflux, 73%; (e) $POCl_3$, DMF, 91%; (f) $(Boc)_2O$, DMAP, MeCN, quant.; (g) $NaBH_4$, MeOH, 0 °C to room temperature, 92%; (h) Br_2, PPh_3, cyclohexane, 93%; (i) pyrrolinone **146**, NaH, DMF, 0 °C to room temperature, 52%; (j) $Pd(OAc)_2$ (10 mol%), PPh_3 (60 mol%), Ag_2CO_3 (2 equiv.), NEt_3, PhMe, 110 °C, 74%; (k) $LiAlH_4$, THF, reflux, 56%